Phase diagram of a 3D, gauge fermion scalar model with compact U(1) gauge symmetry

Marc-Antoine Senechal

Thesis submitted to the University of Glasgow for the Degree of Master of Science in particle physics.

Department of Physics and Astronomy, University of Glasgow, June 1997

ProQuest LLC.
789 East Eisenhower Parkway
P.O. Box 1346
Ann Arbor, MI 48106 – 1346

Acnowlegements

I thank Dr Iain Barbour who proposed me this particular research topic and supervised my work with great patience and kindness.

I am also very grateful to Dr Andrew Davies, who arranged my stay, and to Nektarios Psycharis as well as Dr Wolfgang Franzky from the Institut fűr Theoretische Physik at Aachen who provided me with the most invaluable advices.

Finally I would like to thank Susan Morisson, Paul Mac Callum and Mark Gibson who have always been willing to help me with my English and computing difficulties.

This thesis is dedicated to Martin Lyon.

Abstract

One of the current concerns for particle physisists is to find out the origin of particle masses in the context of gauge field theories. Certain studies on the close connection that exists between mass generation and spontaneous symmetry breaking have led to an important breakthrough (the Higgs mechanism) but our understanding of the underlying phenomena still needs to be improved. Apparently the origin of particle mass lies outside the foundations of the standard model itself and therefore a satisfactory explanation has to be found beyond this framework.

The development of lattice gauge theories in the last thirty years has permitted exploration of new situations that one could not consider before. It has been shown that at strong gauge coupling a spontaneous breakdown of chiral symmetry arises dynamically. This suggests that the process of fermion mass generation could in fact begin with an interaction between fermion and gauge fields.

This thesis consists of a review of the different elements which compose this search and a presentation of a research performed on a viable alternative model for fermion mass generation.

In the first part the basics of lattice gauge theory will be introduced. The second part outlines the elements of fermion mass generation process and reviews the results obtained so far. The research which is then presented in the third part is concerned with a lattice gauge theory which displays a so-called *shielded gauge* mechanism of dynamical fermion mass generation. This mechanism which assumes some scalar field in addition to the fermion and gauge fields might be retained in the continuum limit, as the lattice spacing shrinks to zero (it displays a second order phase transition). This raises the hope to elaborate a realistic theory with dynamically generated fermion mass in the continuum.

The main purpose of the work presented here was to study the model, for a compact U(1) symmetry, on a three dimensional lattice and to draw its phase diagram. A method inspired by Lee and Yang has been used. It consisted of analysing the distribution of the zeros of the canonical partition function and their response to a change in the hopping parameter and/or the coupling constant. The partition function is expressed as a polynomial in the fermion mass and a Hybrid monte-Carlo scheme is used to generate thermalised configurations at various value of β and κ. The coefficients of the corresponding polynomial are extracted via a Lanczos algorithm and the zeros are then found by a standard root-finding routine. The theorem of Lee and Yang allows us to locate the phase transitions. In order to perform a finite size scaling analysis of the zeros several simulations were made on 4^3, 6^3, 8^3 and 10^3 lattices. This led to the determination of critical exponents which give the order of the phase transitions as well as their related universality class.

Contents

Part I

Introduction

Chapter 1

Lattice Gauge Theories

1.1 Introduction, The need for a new regularization scheme

One of the principal tasks of modern quantum field theory is to establish new non-perturbative approaches. This need to go beyond perturbation theory came from the remaining uneasiness of renormalization procedures and particularly the fact that the confinement of quarks and chiral symmetry breakings couldn't be entirely described with perturbative techniques.

The regularization scheme on a lattice has been proposed by Kenneth Wilson in 1974 [6] and will be outlined as follow: Starting from the path integral formalism we temporary discretize both space and time on a lattice of points. The ultraviolet divergences are thus removed while the discretization of the symmetry groups and the limited number of degree of freedom allows an effective utilization of numerical simulations. These methods of investigation are also encouraged by the fact that the Euclidean version of the path integral formalism discloses a remarkable correspondence between lattice gauge theory and the statistical physics of magnets and fluids. Thus the results obtained on the lattice can be taken over by powerful methods which were elaborated for the studies of statistical systems.

1.2 Construction

1.2.1 Functional integrals in the Euclidean space

The most suitable way to handle complex systems that occur in a gauge field theory is to express them in a path integral formalism. The generating functional

for vacuum diagrams, also called the partition function, is defined by the relation

$$\mathcal{Z} = \int D\psi e^{\imath S} = \int D\psi e^{\int \imath dt \int d^3x L} \tag{1.1}$$

where the integration is taken over all the possible field configurations.

In order to discretize the theory on a lattice we first transfer expression(1.1) to an Euclidean space time where measures are all real. To do so we perform an analytical continuation of the time variable: $t_4 \rightarrow \imath x_4$ - This is known as a Wick rotation. It has the further advantage to "damp" the integrand for those widely oscillating paths which would render numerical simulations quite unreliable. Finally this operation brings the formal connection with statistical mechanics: in its Euclidean version the probability weight (e^{-S_E}) is formally equivalent to the Boltzmann factor.

1.2.2 The regularization procedure

The ultraviolet divergences caused by large momenta do not take place when both space and time are discretized on a lattice. The lattices which are employed are usually hyper-cubical. They can be mathematically defined through the relation

$$L = aZ^4 = \{x| \quad x_\mu/a \in Z\} \tag{1.2}$$

a corresponds to the spacing between two neighbouring sites of the lattice and is referred to as the lattice constant. Since it is the shortest non-zero distance, a momenta cut-off appears automatically, just as a natural consequence of the spectral decomposition of the fields: Writing $x = na$ where n is an integer, the expression of the Fourier transform of $\psi(na)$ is

$$\psi(na) = \int_{-\frac{\pi}{a}}^{\frac{\pi}{a}} \frac{dk}{2\pi} \overline{\psi}_a(k)\, e^{ikna} \tag{1.3}$$

Because of its periodicity in momentum space the theory remains entirely described if we restrain the momenta to be in the range $B = [-\frac{\pi}{a}, \frac{\pi}{a}]$ - called the Brillouin zone. This is how the problem of ultraviolet divergences is directly removed, there is no contribution from the short wavelengths in the perturbation series.

1.2.3 Fields and gauge transformation on the lattice

The particles are restrained to lie on the sites of the lattice. It means mathematically that the matter fields are defined for $x_\mu \in Z$ only. As a consequence of this, all the usual operations that one may perform on ψ are discretized.

The derivative operations for example can be defined as

$$\begin{aligned} \partial_\mu^{Forward}\psi(x) &= \tfrac{1}{a}[\psi(x+a\hat{\mu}) - \psi(x)] \\ \partial_\mu^{Backward}\psi(x) &= \tfrac{1}{a}[\psi(x) - \psi(x-a\hat{\mu})] \end{aligned} \tag{1.4}$$

$\hat{\mu}$ is the unit vector in the direction indicated by μ $(= 1,2,3,4)$. Consequently the hermitean lattice Laplacean in 4 space-time dimension is

$$\Box\psi(x) = \sum_\mu \partial_\mu^F \partial_\mu^B \psi(x) = \frac{1}{a^2}[\psi(x+a\hat{\mu}) + \psi(x-a\hat{\mu}) - 2\psi(x)] \tag{1.5}$$

The gauge transformations of the matter fields, being local, are naturally defined on the lattice sites too. They take the usual form:

$$\psi(x) \to \psi'(x) = \Lambda^{-1}(x)\psi(x) \tag{1.6}$$

Then gauge fields are introduced in order to ensure the invariance of the action (its kinetic part) under equation(1.6). It is particularly interesting to note here how the basic distinction between gauge fields and matter fields is displayed on a lattice theory: Whereas matter fields are exclusively defined on the lattice (defined as an ensemble of point), the gauge fields are in fact associated to the links between these points. This is a direct consequence of their intrinsic role of parallel transporter.

Let define these quantities more precisely. Consider a point x of the lattice and $x + a\mu$ the nearest neighbouring point that one can find in the μ direction. With the corresponding link l we will associate a *link variable* $U(l)$ which is defined as being an element of a given gauge group G.

$$U(l) = U(x + a\hat{\mu}, x) = U_{xy} \in G \tag{1.7}$$

U_l is defined to be unitary and therefore expressible as the exponential of an imaginary matrix

$$U(x + a\hat{\mu}, x) = \exp(\imath a g T_b A_\mu^b(x) \tag{1.8}$$

where g is the coupling constant, T_b the generator of the gauge group (hence an Hermitean traceless matrix) and A^b_μ is the gauge field. Under the local gauge transformation that equation(1.6) introduced for the matter fields, these link variables will transform as

$$U'(y,x) = \Lambda^{-1}(y)U(y,x)\Lambda(x) \tag{1.9}$$

which is the usual transformation law for parallel transporters. Hence let's imagine a particle which follows a straight curve from x to dx. Whenever the parallel transporter will deviate infinitesimally from the Unit matrix it will automatically generate a gauge field. This field embodies the dynamics, so to speak, which in fact balance the deviation. The generation of the gauge field by U appears quite clearly if we consider the series expansion of equation(1.8) when it tends to the continuum: as the lattice spacing a tends to zero we get

$$U(x + a\mu, x) = 1 - aA_\mu(x) \tag{1.10}$$

where $A_\mu(x)$ is the *Lie algebra valued* vector: $A_\mu(x) = -\imath g T_b A^b_\mu(x)$.

In order to make the action invariant under the local gauge transformation we can define the covariant derivative as

$$\begin{aligned} D^F_\mu\psi(x) &= \tfrac{1}{a}[U^{-1}(x,\mu)\psi(x + a\mu) - \psi(x)] \\ D^B_\mu\psi(x) &= \tfrac{1}{a}[U(x,\mu)\psi(x) - \psi(x - a\mu)] \end{aligned} \tag{1.11}$$

Applying equations (1.6) and (1.9) to this quantity one notes that D_μ transforms covariantly in the sense

$$D'_\mu\psi'(x) = \Lambda^{-1}(x)D_\mu\psi(x) \tag{1.12}$$

The invariance of the action is then assured by mean of the gauge fields. If we consider equation (1.10) within, say, the backward covariant derivative :

$$\begin{aligned} D^B_\mu\psi(x) &= \tfrac{1}{a}\left((1 - aA_\mu(x))\psi(x) - \psi(x - a\mu)\right) \\ &= \left(\partial^B_\mu - A_\mu(x)\right)\psi(x) \end{aligned}$$

The principle is the same as for the continuum gauge theory. Since Observables have to be gauge invariant functions of the basic variables it seems worthwhile to point out that such quantities can be constructed from expressions of the form $\sum_{<xy>} \psi(x)U(x,y)\psi(y)$. There is a second type of "elementary" gauge invariant quantity that will be introduced in the next paragraph.

1.2.4 Action of a theory on the lattice

On the lattice there are several different ways of expressing the Action for a given theory, the basic requirements on S being just that it is gauge invariant, that it recovers the initial theory as we approach the continuum limit and usually that it is local. The main examples will be provided as we will introduce the action of the gauge-fermion-scalar model which is investigated in the third part of this thesis.

As a first illustration of the discussion above we introduce the Wilson Action which describes a pure gauge theory.

It is obtained by tracing U_l around each plaquettes *i.e.* around each smallest closed loops that we can find on the lattice. They consist on four links and the corresponding parallel transporter is therefore

$$U_p = U_l(x, x + a\hat{\nu})U_l(x + a\hat{\nu}, x + a\hat{\mu} + a\hat{\nu})U_l(x + a\hat{\mu} + a\hat{\nu}, x + a\hat{\mu})U_l(x + a\hat{\mu}, x) \quad (1.13)$$

The action is then defined in terms of these *plaquette variables* U_p

$$S_G = \sum_p S_p(U_p) \quad (1.14)$$

where

$$S_p(U_p) = -\beta\{\frac{1}{2Tr1}(TrU + TrU^{-1}) - 1\} \quad (1.15)$$

Several types of action can be constructed but this particular formulation is the most simple. It also has the advantage to be real and positive.

The most important matter is the evolution of such expressions as we return to the continuum limit. This leads to the second part of this section which concerns the formal analogies that has been identified between gauge theories on the lattice and statistical mechanics. It allows one to use the experience accumulated in statistical physics in order to investigate how the main quantities behave as the lattice spacing tends to zero. This feature really played an essential role in the success of the whole regularization procedure.

1.3 Toward the continuum limit

Finding the path from a given lattice gauge theory to its continuum limit is a difficult task whose success is not assured. When the lattice spacing a is smoothly

brought to zero, in addition to find a suitable renormalization procedure as the ultraviolet divergences reappear, one has to monitor the evolution of the lattice measurables which were all defined with respect to a. All these quantities must remain finite and independent of the lattice spacing as this last tends to zero.

In practice, the search for a continuum limit requires the tuning of certain parameters (in the following we will be particularly concerned with the tuning of the coupling constant). It turns out that this tuning is analogous to the tuning performed within statistical models in the approach to a critical temperature. Some powerful methods designed for this purpose in statistical mechanics will then be applied on the lattice [8].

In order to illustrate how a correspondence with statistical mechanics could arise let consider how interactions take place on the lattice. They are acting via the link variables: To each gauge-link variable is associated an elementary interaction which extends over a distance of order a. By all means they have to be correlated in order to cover distances involved in real processes. For example we know that the typical range of strong interactions is about one fermi.

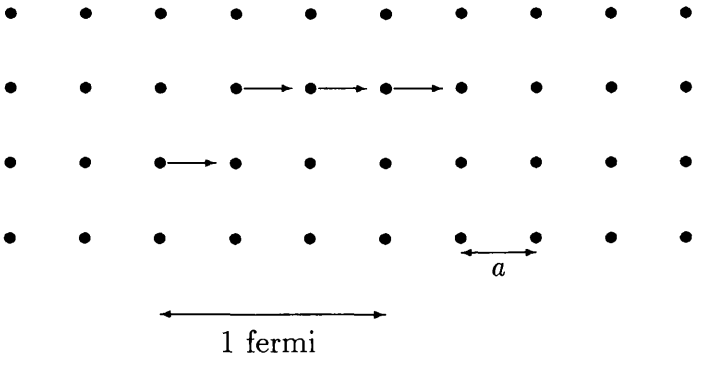

When the lattice spacing is narrowed one fermi will correspond to a greater number of sites. Hence the alignment of the elementary interactions, their cooperation, must be observed over a larger number of sites.
Ultimately in the continuum limit this *correlation length* has to be infinite.

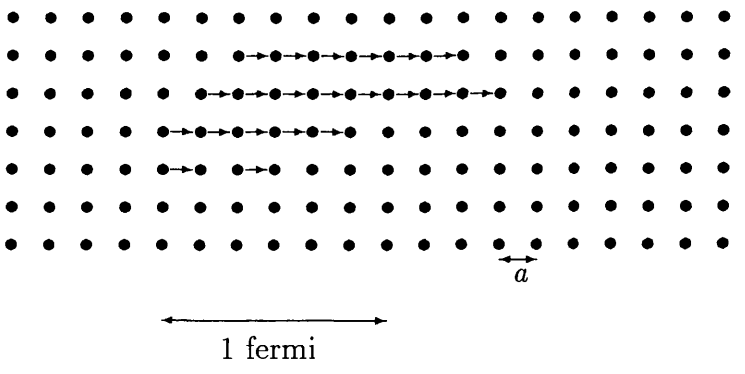

As will be shown in the next section, statistical physics introduces some quantities which are very relevant for the study of these phenomenon. The correlation functions for instance corresponds exactly to the quantities that we need to monitor in the problem above. Moreover the theory of critical phenomena explains how there exists certain situations where the correlation length becomes precisely infinite and therefore allows the shrinkage of the lattice spacing to zero.

1.4 Related elements of statistical physics

The partition function

The partition function Z is initially introduced within the key equation of statistical mechanics as a normalization factor . Considering a system in equilibrium and which can be in N possible states. The probability for this system to have an energy E_n is given by the equation

$$P = \frac{1}{\mathcal{Z}} e^{-\frac{E_n}{kT}} \tag{1.16}$$

where k is the Boltzmann constant, T the temperature and $\mathcal{Z} = \sum_{n=1}^{N} e^{-\frac{E_n}{kT}}$.

In fact Z contains all the information required about the thermodynamics quantities.

Mathematically we have

$$\text{Free energy:} \qquad F = -(\tfrac{T}{V}) \ln \mathcal{Z}$$

$$\text{Internal energy:} \qquad U = -T^2(\tfrac{\partial}{\partial T})(\tfrac{F}{T}) = -(\tfrac{\partial}{\partial \beta})(\tfrac{\ln \mathcal{Z}}{V}) \tag{1.17}$$

$$\text{Specific heat:} \qquad C = (\tfrac{\beta^2}{V})(\tfrac{\partial^2}{\partial \beta^2}) \ln \mathcal{Z}$$

Consequently if the partition function is known all the thermodynamical properties of the system can be found.

Phase transitions

The quantities above can display, at a given temperature T_C, singularities which are manifested in experiments by phase transitions in the system. The order of a transition depends on which derivative the Free energy shows the singularity: a first order phase transition will be observed if there is a discontinuity in the first derivative of F (*i.e.* U) and similarly a second order phase transition will be observed whenever there is a discontinuity in C.

This last kind of phase transition is a crucial matter for our search for a continuum limit. It is associated, by definition, to the divergence of the correlation length which was mentioned in section(1.3).

An other characteristic of a second order phase transition is related to the fact that it makes the separation between two different states of symmetry within the system [7]. In fact the symmetry is reduced as we pass below the critical temperature T_c. Because of this reduction of symmetry, an additional parameter is needed to describe the thermodynamics in this phase. This parameter known as the *order parameter* is an extensive variable generally accessible to measurement (for example in a ferromagnetic it is the magnetization vector) and it is generally its own correlation length which diverges in the vicinity of T_c.

The Correlation function

Let's consider the spin S_i of an electron in a given system: interactions favour the alignment of spins and a nearby spin S_j will tend to assume the same orientation as S_i. However thermal agitation counteracts this tendency and exerts a decorrelating effect (For future reference, models which study the

collective behavior of electrons spin on a lattice are referred to as *Ising models*): The correlation function $< S_i S_j >_c$ is a measure of the influence that S_i actually exerts over S_j. It is defined by the relation

$$< S_i S_j >_c = < S_i \cdot S_j > - < S_i >< S_j > \tag{1.18}$$

In the present case if $< S_i S_j >_c$ is small it then induces that thermal agitations get the upper hand over the correlating influence of S_i.

The range of the influence exerted by S_i over its neighbourhood is measured by the correlation length which is intrinsically related to the correlation function. It has been showed that $< S_i S_j >$ decreases exponentionally with the distance $|i-j|$. Expressed in lattice units, the correlation length ξ is then given by

$$< S_i S_j >= e^{\frac{-a|i-j|}{\xi}} = e^{\frac{-r_{ij}}{\xi}} \tag{1.19}$$

An other important feature established by statistical theory is how the correlation length depends on the temperature. For example we have in the case of the one-dimensional Ising model: $\xi = \frac{a}{|\ln \tanh \frac{J}{kT}|}$ where J is a coupling constant.

The situation is more complex in the case of Gauge interactions. However the point remains that one can find a critical temperature T_c at which the correlation length diverges. As a result of this the correlation function will become *scale invariant i.e.* its mathematical expression will not contain any characteristic length anymore.

Critical phenomena

Considering the system of the previous paragraph, one can observe that the correlation between electrons spins gives rise to some clusters inside which the electrons are either all spin-up or all spin-down. These clusters have variable size and they may be embedded into each others. For example one could find a small island of 'spin-ups' lying inside a bigger region of 'spin-downs'. The range of possible size is closely connected to the correlation length whose order gives somehow the average size of these clusters.

As the temperature is lowered toward T_c, ξ grows and consequently the sizes of the clusters can get much more diverse. At $T = T_c$ the correlation length becomes infinite. Thus the fluctuations extend over regions of all possible dimensions: there is no scale of length anymore. In geometrical terms, one says that

the system displays a fractal structure.

Hence having started with short-range interactions (between nearest neighbours) at a second order phase transition we find correlations of *infinite* range. Moreover this large-scale cooperative phenomenon gives rise to a second remarkable feature. Indeed some important properties of the system do not depend on the details of the interactions anymore. We find some *universal* quantities whose measurement give the same value in several different theories provided that they share, for example, the same dimensionality or interaction symmetries.

Consider for example the specific heat C introduced in equation(1.14). It has been established from experimental observations that in the vicinity of the critical point it displays the singular behavior

$$C \sim (T - T_c)^{\alpha} \tag{1.20}$$

α is a critical exponent and it has the same value for all the theories sharing the same "universality class". These emerging similarities between different theories can then lead us to fruitful comparisons. We can even work out a convenient lattice regulator to perform our tuning by working on an other, simpler, theory provided it belongs to the same universality class as our theory of interest.

Part II

Generating the mass of the fermions

Chapter 2

General principles related to the fermion mass generation

2.1 Introduction to the problem

We mentioned earlier that the Standard Model was a significant breakthrough of quantum field theory. It not only presents a united description of electromagnetic, weak and strong interactions: its predictions are in outstanding agreement with every data obtained experimentally.

However some areas of this successful, perturbatively renormalizable, theory remain poorly understood and so far its improvement unavoidably requires the introduction of some arbitrary, free parameters which by all means deride the initial elegance of the theory. It is now generally admitted that a deeper coherence has to be found beyond the model itself.

One of the major concerns is to find a correct explanation of the origin of the fermions mass. The mass of their particles, determined by experiments, are not predicted by the standard model: it can only accommodate them with its description of fundamental interactions. The main point here is the fact that if we introduced artificially some bare mass terms in the Lagrangian, then they would break its invariance under gauge transformations (the one which characterizes electro-weak interactions). Hence the origin of particle masses raised a thorny problem [1] : How can one develop a realistic theory of massive particles interacting with each other without losing these so compelling gauge schemes?

[1] This difficulty is nonetheless not so surprising since the main weakness of the standard model is that it cannot describe gravitational interactions.

An answer has been found in a *spontaneous breakdown* of the electro-weak symmetry. This important phenomenon - which is observed in many natural processes - rests on the following observation: The Hamiltonian (or the commutation relations) which characterizes a theory could possess an exact symmetry but the physical states which are actually observed might not provide a net representation of this symmetry. More specifically a symmetry of the Hamiltonian might not be a symmetry of the vacuum.

2.2 Role of chiral symmetries

The relation between fermion masses and the unified description of interactions in the standard model has not been understood yet. Nonetheless an interesting feature has been pointed out: If the particles had no mass at all then a larger group of symmetries would be observed.

Chiral symmetries belong to this group and the formal relationship which exists between their breakdown and the generation of fermion masses is naturally an interesting feature to study. It turns out however that the particular intervention of chiral symmetries is not so fortunate: these symmetries are closely related to the gauge symmetry that rules electro-weak interactions. Hence they would rather prevent one from finding a straightforward solution. We cannot intend for example to express the theory in a representation which displays a chiral symmetry and then simply beget its breaking by a suitable "mass term": It would plainly destroy the whole gauge theory and the renormalizability of the Standard Model.

The notion of chiral symmetry is in fact directly connected with the difference which exists between two representations of the Lorentz group: the two spinors which cover spin-$\frac{1}{2}$ particles. A chiral transformation interchanges the so-called right handed and left handed spinors from these two representations. Somehow its effect will then mix with the parity violation displayed by weak interactions.

Let's make to appear explicitely these two spinors, introduced in section(1.2) in the Lagrangian density which describes N free Dirac fermions. We have

$$\mathcal{L} = i\overline{\psi}_k \gamma^\mu \partial_\mu \psi_k - m\overline{\psi}_k \psi_k, \; k = 1, 2, ..., N \tag{2.1}$$

We first note that L is invariant under $U(N)$ transformations:

$$\psi_j \mapsto \psi'_j = [exp(\imath w_\alpha T^\alpha)]_{jk}\psi_k \tag{2.2}$$

where the $T^\alpha = \frac{\lambda^\alpha}{2}$ operators introduce our particular Lie algebra: we have $tr\lambda^\alpha\lambda^\beta = 2\delta_{\alpha\beta}$. Now we use the particular Majorana representation - where all the γ^μ matrices are imaginary . The fermion fields can then be explicitly decomposed into two spinors: the right handed $\psi_{R,k} = \frac{1-\gamma^5}{2}\psi_k$ and the left handed $\psi_{L,k} = \frac{1+\gamma^5}{2}\psi_k$ such that

$$\psi_k = \begin{pmatrix} \frac{1-\gamma^5}{2}\psi_k \\ \frac{1+\gamma^5}{2}\psi_k \end{pmatrix} \tag{2.3}$$

These two spinors field are respectively assigned to the representations $(\frac{1}{2}, 0)$ and $(0, \frac{1}{2})$ of the Lorentz group.
The Lagrangian (2.1) now becomes

$$\mathcal{L} = \imath\overline{\psi}_{Lk}\gamma^\mu\partial_\mu\psi_{Lk} + \imath\overline{\psi}_{Rk}\gamma^\mu\partial_\mu\psi_{Rk} - m\overline{\psi}_{Lk}\psi_{Rk} - m\overline{\psi}_{Rk}\psi_{Lk} \tag{2.4}$$

Hence the kinetic terms leave L invariant under a larger $U_L(N) * U_R(N)$ chiral group. The gauge interactions, by construction, don't affect this symmetry neither but we see clearly that the mass terms mix the two groups. Reciprocally the breaking of a chiral symmetry implies the appearance of new terms in the Lagrangian that can be interpreted as particle masses.

2.3 Phenomenon of spontaneous symmetry breaking

First illustration

We first note that in fact in the process the symmetry is not so much 'broken' as 'secret' or 'hidden'. This occur in many phenomenon of nature. We can find an inspiration of this technique for example in the collective behaviour that occur in a ferromagnetic material (when there is no magnetic field). Its Hamiltonian is rotationally invariant. However if we bring it below the Curie

We first note that L is invariant under $U(N)$ transformations:

$$\psi_j \mapsto \psi'_j = [exp(\imath w_\alpha T^\alpha)]_{jk}\psi_k \tag{2.2}$$

where the $T^\alpha = \frac{\lambda^\alpha}{2}$ operators introduce our particular Lie algebra: we have $tr\lambda^\alpha\lambda^\beta = 2\delta_{\alpha\beta}$. Now we use the particular Majorana representation - where all the γ^μ matrices are imaginary . The fermion fields can then be explicitly decomposed into two spinors: the right handed $\psi_{R,k} = \frac{1-\gamma^5}{2}\psi_k$ and the left handed $\psi_{L,k} = \frac{1+\gamma^5}{2}\psi_k$ such that

$$\psi_k = \begin{pmatrix} \frac{1-\gamma^5}{2}\psi_k \\ \frac{1+\gamma^5}{2}\psi_k \end{pmatrix} \tag{2.3}$$

These two spinors field are respectively assigned to the representations $(\frac{1}{2}, 0)$ and $(0, \frac{1}{2})$ of the Lorentz group.
The Lagrangian (2.1) now becomes

$$\mathcal{L} = \imath\overline{\psi}_{Lk}\gamma^\mu\partial_\mu\psi_{Lk} + \imath\overline{\psi}_{Rk}\gamma^\mu\partial_\mu\psi_{Rk} - m\overline{\psi}_{Lk}\psi_{Rk} - m\overline{\psi}_{Rk}\psi_{Lk} \tag{2.4}$$

Hence the kinetic terms leave L invariant under a larger $U_L(N) * U_R(N)$ chiral group. The gauge interactions, by construction, don't affect this symmetry neither but we see clearly that the mass terms mix the two groups. Reciprocally the breaking of a chiral symmetry implies the appearance of new terms in the Lagrangian that can be interpreted as particle masses.

2.3 Phenomenon of spontaneous symmetry breaking

First illustration

We first note that in fact in the process the symmetry is not so much 'broken' as 'secret' or 'hidden'. This occur in many phenomenon of nature. We can find an inspiration of this technique for example in the collective behaviour that occur in a ferromagnetic material (when there is no magnetic field). Its Hamiltonian is rotationally invariant. However if we bring it below the Curie

temperature T_c the ground state of the system develops a non-zero magnetization $\vec{M}$ and therefore loses its invariance under rotations. The direction of $\vec{M}$s has been selected "spontaneously" by the system as it cooled and this is why the symmetry is said to be spontaneously broken.

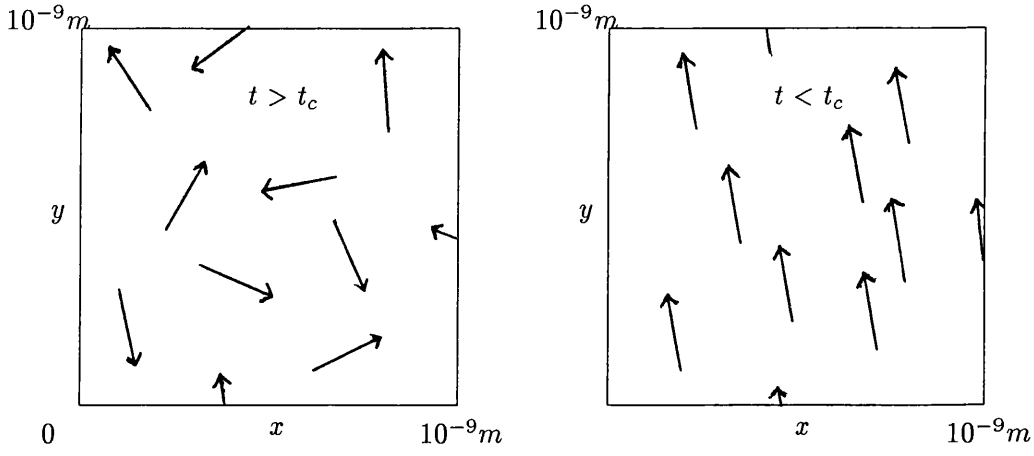

Figure 3.1: On the microscopic level: we see elementary magnetic moments which arise from the spin of the electrons[2]*. Although they tend to align with each other thermal fluctuations refrain them to do so unless the temperature fall below* t_c [3].

We will now consider this phenomenon in the context of quantum field theory. Thus the state of lowest energy (the ground state) is the vacuum state and the rotational symmetry of the ferromagnet is generally replaced by an internal symmetry of the field. The spectra of small oscillations around the vacuum state can also be connected to particle masses.

The first method is to postulate the existence of a field having a non-zero value in the vacuum. In terms of a field operator $\hat{\varphi}(x)$ we write

$$\varphi_c(x) = < 0|\hat{\varphi}(x)|0 > \neq 0 \tag{2.5}$$

We note that this field has to be scalar since the vacuum is rotationally invariant.

[2]see section(1.4)

[3]This process is in fact more complex and requires advanced elements of statistical mechanics

Case of a global symmetry

As a formal example we consider the Lagrangian of a complex scalar field theory,

$$\mathcal{L} = (\partial_\mu \varphi)(\partial^\mu \varphi^*) - V(\varphi, \varphi^*) \tag{2.6}$$

with a potential of the form

$$V(\varphi, \varphi^*) = \mu^2 \varphi\varphi^* + \lambda(\varphi\varphi^*)^2 \tag{2.7}$$

This Lagrangian is then invariant under a global U(1) gauge transformation.

$$\varphi(x) \mapsto \varphi(x)' = e^{-iq\Lambda}\varphi(x) \tag{2.8}$$

$$\varphi^*(x) \mapsto \varphi^*(x)' = e^{iq\Lambda}\varphi^*(x) \tag{2.9}$$

If both μ^2 and λ are positive then the potential has only one (trivial) absolute minimum at $\varphi_c = 0$ which corresponds to the conventional vacuum. However if we take $\mu^2 \leq 0$ this minimum occurs at a non-zero value of φ (λ must remain positive to ensure that the potential is bounded from below). We have

$$|\varphi_c|^2 = -\frac{\mu^2}{2\lambda} \tag{2.10}$$

Hence there is a circle of minima for this potential and the true vacuum state of the system has to be one of these states. Once φ_c has been manifested, the U(1) symmetry does not hold anymore in the sense that a rotation of the vacuum state would lead to a different state. φ_c is not invariant under U(1). Let's denote the particular phase of the vacuum δ and rewrite the theory as expanding about this state. We reexpress φ_c in the form $\varphi_c = \frac{1}{\sqrt{2}} v e^{i\delta}$, where $v = \sqrt{\frac{-\mu^2}{\lambda}}$. We can then introduce a field redefinition:

$$\varphi(x) = \frac{1}{\sqrt{2}}(\rho(x) + v)e^{i[(\frac{\xi(x)}{v})+\lambda]} \tag{2.11}$$

This leads to rewrite the Lagrangian

$$\mathcal{L} = \frac{1}{2}[(\partial_\mu \rho)^2 + \frac{1}{2}[\frac{(\rho + v)}{v}]^2(\partial_\mu \xi)^2 + \mu^2\rho^2 - \lambda v \rho^3 - \frac{\lambda\rho^4}{4} - \frac{1}{4}\mu^2 v^2. \tag{2.12}$$

This Lagrangian clearly describes two real fields, ρ and ξ, one massless and the other massive with a real positive mass $-\lambda v^2$. The massless state is a Nambu-Goldstone boson; its occurrence is a characteristic of a the spontaneous breakdown of a continuous symmetry and is stated by the Nambu-Goldstone theorem.

Although this Lagrangian describes the same theory as in eq (2.6) it is not $U(1)$ symmetric. We see why some prefer to describe the symmetry as 'secret' or 'hidden': Someone which is not aware of the previous field redefinition would probably assume that the Lagrangian is just not invariant under phase changes. However the particular coefficients of the non-invariant terms are such that we can recast the Lagrangian in a symmetric form.

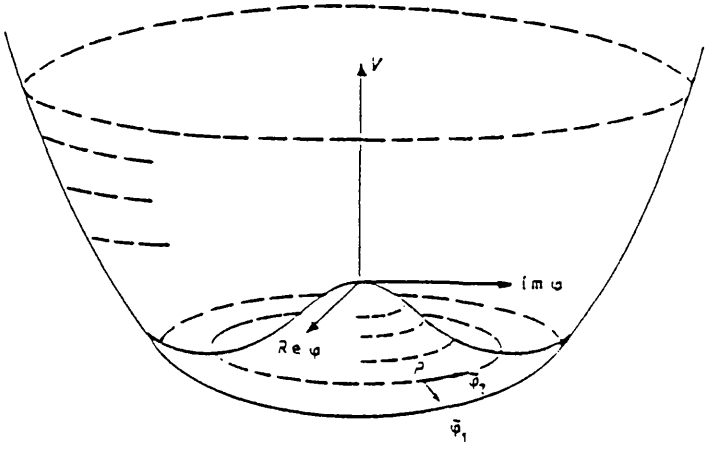

Figure 3.2: The potential energy density $V(\varphi)$ increases quadratically in the radial plane ($\varphi_2 = 0$). Thus the displacement associated with ξ induces a quantum excitation which correspond to a massive particle. On the other hand ρ goes in the "valley" where V is constant and the goldstone boson is therefore massless.

Chapter 3

Mechanisms of mass generation

3.1 Review of the Higgs mechanism

3.1.1 Description

The Higgs mechanism implements the previous technique to the more difficult, but richer, case of local symmetry transformations. As a result it provided a suitable description of particle masses for the standard model.

When we consider a complex scalar field invariant under a *local* gauge transformation we must implement the Lagrangian of eq(2.6) by introducing a covariant derivative $D_\mu = \partial_\mu - \imath g A_\mu(x)$. We must also introduce a kinetic term (we take $[-\frac{1}{4}F_{\mu\nu}F^{\mu\nu}]$) for the vector field $A_\mu(x)$.

Once again if μ^2 is negative the vacuum state lies away from the origin and this leads to the reparameterisation introduced in equation(2.11). However in this case the covariant derivative of the field φ will also introduce a mass term for the vector field $[\frac{1}{2}g^2v^2A^\mu A_\mu]$. Another term arises which can be interpreted if we perform the field redefinition:

$$B_\mu(x) = A_\mu(x) + \frac{1}{gv}\partial_\mu\xi(x) \tag{3.1}$$

where $\xi(x)$ is a boson field as introduced in eq(2.11). We don't carry out explicitly these calculations here. We just mention that the Lagrangian then describes explicitly a massive vector field B_μ and a massive scalar field ρ with respective masses

$$\begin{aligned} m_B &= gv \\ m_\rho &= \sqrt{-2\mu^2} \end{aligned} \tag{3.2}$$

From the three spin components of the vector field, two are supplied by the original gauge field A_μ and the third, the longitudinal component, is supplied by the would-be Goldstone boson ξ. These features are the main hallmarks of the Higgs mechanism.

We can get another insight of how it worked if we consider the procedure from the following angle: Since under a local gauge transformation the field φ transforms as $\varphi \to \varphi e^{ig\alpha(x)}$, it is possible to transform away the Goldstone boson $\xi(x)$ in equation(2.11) by choosing $\alpha(x) = \frac{\xi(x)}{vg}$. However it brings the vector field to transform as $A_\mu(x) \to A_\mu(x) + \partial_\mu \frac{\xi(x)}{vg}$ which is in fact the field redefinition of equation(4.1).

Hence equations (2.11) and (3.1) can be regarded as a local gauge rotation of the theory. Since it transformed away the Goldstone bosons, this last is not a physical field. Another point to mention is that important quantities such as the Noether current (relating to the usual conservation of charges) are conserved. Thus despite its "spontaneous breakdown" the symmetry remains with many respects exact.

3.1.2 Limits of the theory

The Higgs mechanism provides a comfortable, perturbatively renormalizable, way to introduce particle masses in gauge field theories. However if it describes the fermion mass generation phenomenologically it does not truly predict these masses: They simply appear as arbitrary, free parameters which depend on our field redefinition.

Some other features are also disappointing. For example the scale of the fermion masses, set by the scale of the electro-weak symmetry breaking, is much larger than the scale which has been actually measured: Only the top quark does have an "heavy" mass which seems consistent with the results of the theory. The model doesn't explain either why there are three different generations of fermions. Finally one has to remember that the Higgs field has been postulated but its existence has never been confirmed by experiments. The fact for example that its renormalized square mass would be contrived to be negative leads to view the Higgs mechanism as an artificial feature of the standard model [10].

We will now see non-perturbative methods which have been developed recently. In particular the fermion-gauge models which display at strong gauge

coupling a spontaneous chiral symmetry breaking of dynamical origin suggest the existence of interesting alternatives to the Higgs mechanism.

3.2 The dynamical mass generation alternative

In quantum mechanics terms, a spontaneous symmetry breakdown is exhibited by the non-zero vacuum expectation value for some field operator that we called the order parameter $\mathcal{P}$ (in reference to the phase transition that is manifested in statistical physics). In the Higgs mechanism this last corresponds to the vacuum expectation value of the *elementary* Higgs boson field.

It is important to note that $\mathcal{P}$ does not need in fact to be linear in the elementary fields. The Goldstone theorem holds as well if the order parameter arises as a composite state of those fields. The problem in this case is that usual approximations fail completely - precisely because of the non-linearity of $\mathcal{P}$ in the field quantities. One must therefore uses non-perturbative approaches.

Nambu and Jona-Lasinio were the first to propose the idea of dynamical symmetry breaking: they defined a model where the order parameter was generated by the interactions between nucleons and pions [11]. The model is defined by a 4-fermion interaction Lagrangian in d=1+3

$$\mathcal{L} = i\overline{\psi}\ \partial\!\!\!/\psi + \frac{1}{2}g^2[(\overline{\psi}\gamma_\mu\tau\psi)^2 - (\overline{\psi}\gamma_5\tau\psi)^2] \tag{3.3}$$

where τ are isospin matrices. They showed that if the coupling g^2 is above a certain value then a mass is generated *dynamically*: The order parameter results from the interactions between the elementary fields. In their particular model, the exact chiral $SU(2)_L \times SU(2)_R$ symmetry is then broken to $SU(2)_V$ and this produces a massless triplet of pseudo-scalars, as bound states, that one could identify as idealized pions.

Since then, numerous investigations of various strongly coupled gauge theories have been carried out on the lattice. They revealed that dynamical mass generation is a general property of these theories. It does not only occur in QCD but also in QED at strong coupling. Therefore Dynamical Symmetry Breaking is seriously considered as a mean to construct new mechanisms of fermion mass generation. They are particularly appealing since they would avoid the *introduction* of a fundamental scalar field. The Higgs boson, should it exist, would be

interpreted as a composite state, formed by some strong coupling beyond the standard model itself. The following chapters concern the study of one of these new models.

Chapter 4

Fermion-gauge-scalar model on the lattice

4.1 Introduction

Dynamical chiral symmetry breaking turns out to be a general property of strongly coupled gauge-fermion theories studied on the lattice. The experience accumulated since twenty years has then permitted to study some interesting mechanisms of dynamical mass generation. Hence the main issue now is rather to define a realistic continuum model from lattice gauge theories.

The model which will be presented in this section exhibits the hallmarks of dynamical symmetry breaking: The chiral symmetry is spontaneously broken once interactions between fermion and gauge fields have generated a bound state whose vacuum expectation value is non-zero. Massive physical fermion states are then observed in the spectrum as well as the massive Goldstone boson. The main interest of this model comes from the fact the mechanism on which it rests could work as well in the continuum limit. It assumes a scalar field [1] which leads to restore the chiral symmetry - at certain values of the gauge coupling and of its propagator[2] - in such a way that the transition between the two phases (the one where the chiral symmetry is broken and the one where it is restored) is of second order. If the model is non-perturbatively renormalizable in this region then it could truly describe realistic massive fermions in the continuum and be

[1] This does not however look like the Higgs mechanism. Here the scalar field is confined by the gauge field.

[2] The propagator of the scalar field is monitored through the hopping parameter κ which will be introduced in the action of the theory in section(4.3.1).

an alternative to the Higgs mechanism.

4.2 The shielded gauge mechanism

This mechanism of dynamical mass generation rests on the interaction between a confining gauge field U, which belongs to some representation of a compact gauge group G, and a fundamental fermion field χ. It gives rise to a fermion condensate *i.e* a fermion bound-state whose vacuum expectation value $< \overline{\chi}\chi >$ becomes non zero at strong gauge coupling[17]. In the corresponding region of the phase diagram a spontaneous breaking of the chiral symmetry is then observed. This particular mechanism makes use of a fundamental scaler field ϕ whose role is twofold:

First it gives rise to some composite physical fermion states, of the form $F = \phi^{\dagger}\chi$, which are G-neutral. Therefore they don't undergo the confinement induced by the gauge charge and can exist asymptotically (this feature is at the origin of the name of the mechanism). In the chirally broken phase, the fermion mass m_F is observed to be non-zero and we then have a dynamical mass generation. Goldstone bosons are also present: they are composed of χ and $\overline{\chi}$.

The second role of the scalar field is to lead to restore the Chiral symmetry, as κ increase, in such a way that this occurs smoothly in the scaling region of a second order phase transition. The mass of the fermions then scales progressively to zero.

4.3 Abelian case with a compact U(1) gauge symmetry

In the work presented in the second part of this thesis, the shielded gauge mechanism has been applied to the compact U(1) gauge group. It is thus concerned with the study of Abelian models - such as compact QED in the limit case where scalar fields are damped.

One can thus identify the fermion condensate with an electron-positron pair while the coupling constant refers to the electric charge and the Wilson action (introduced in equation(1.11)) is related to the electromagnetic field. A great

interest is devoted to this model[19] since it displays important properties. After having introduced the action of the theory we will discuss its different subsystems as well as the results obtained so far in previous works.

4.3.1 Action of the $\chi U \psi$ model

The model is defined on an Euclidean hyper-cubical lattice. The link variables are elements of the compact gauge group U(1) and we can express them in terms of the Abelian gauge fields A_μ through the relation:

$$U_{xy} = \exp(\imath e A_\mu(x)) \tag{4.1}$$

Here $A_\mu(x)$ is a real number corresponding to the continuum vector potential $(A_\mu(x) = aA(x)_\mu)$ and e is the bare (electromagnetic) gauge coupling.
The sum over plaquettes of these link gauge variables leads to the Wilson action introduced in section(1.2.4). The gauge group being compact $U(1)$, it takes the form

$$S_U = \beta \sum_p [1 - ReU_p] \tag{4.2}$$

$\beta = \frac{1}{ae}$ And U_p represents the plaquettes product.

Since we are concerned with chiral symmetries we want this gauged fermionic part of the action to conserve at least some traces of them on the lattice. It will be then discretized by means of the staggered fermion scheme. The fermion doubling problem is overcome by performing a Kawamoto-Smit transformation: Starting from the naive fermion action

$$S = \frac{1}{2} \sum_{x,\mu} [\overline{\psi}(x)\gamma_\mu \psi(x+\mu) - \overline{\psi}(x)\gamma_\mu \psi(x-\mu)] + m \sum_x \overline{\psi}(x)\psi(x) \tag{4.3}$$

We operate a spin diagonalization, using a local change of variables of the form: $\psi(x) = T(x)\chi(x)$.
$T(x)$ is required to be unitary and such that $T^\dagger(x)\gamma_\mu T(x+\mu) = \eta_\mu(x) I$.
We choose $T(x) = \gamma_1^{x_1}\gamma_2^{x_2}...\gamma_4^{x_4}$ and then the action becomes

$$S = \frac{1}{2} \sum_{x,\mu,\alpha} \eta_\mu(x) \{\overline{\chi_\alpha}(x)\chi_\alpha(x+\mu) - \overline{\chi_\alpha}(x)\chi_\alpha(x-\mu)\} + m \sum_{x,\alpha} \overline{\chi_\alpha}(x)\chi_\alpha(x) \tag{4.4}$$

Where the phase factor is $\eta_\mu = (-1)^{x_1+x_2+...+x_{\mu-1}}$ ($\eta_1 = 1$). Since we got rid of the γ_μs, S can run in principle over any number of possible values of the spinor

indices $\alpha = 1, 2, ..., k$. For instance we take the minimal choice, $k = 1$, (we will then omit this trivial index) and the coupling to the gauge fields leads naturally to a first expression

$$S_\chi = \frac{1}{2}\sum_x \overline{\chi}(x)\sum_{\mu=1}^{4}\eta_{\mu x}(U_{x,\mu}\chi_{x+\mu} - U^\dagger_{x-\mu,\mu}\chi_{x-\mu}) + am_0\sum_x \overline{\chi}_x\chi_x \tag{4.5}$$

Although the degeneracy is only partially removed, this 'discrete' action keeps trace of residual chiral symmetries and we expect to get back in the continuum limit the global chiral symmetry $U(N_f)*U(N_f)$ (where N_f is the number of fermion species found in this limit).
χ has a unitary charge. The bare fermion mass m_0 has been introduced for reasons that will be explained in chapter 6 and the realistic situation is meant in the limit $m_0 = 0$.

The scalar part of the action does not require special techniques of discretization and we just introduce the following bilinear expression in the scalar fields which is gauge invariant:

$$S_\phi = -\kappa\sum_x\sum_{\mu=1}^{4}[\phi^\dagger_x U_{x,\mu}\phi_{x+\mu} + \phi^\dagger_{x+\mu}U^\dagger_{x,\mu}\phi_x] \tag{4.6}$$

The hopping parameter κ is related to the bare mass of the scalar fields and plays its most important role in the renormalization procedure.

We can now gather all the different parts of the action:

$$\boxed{\begin{array}{c} S = S_U + S_\chi + S_\phi \\ \\ S_U = \beta\sum_p[1 - Re\{U_p\}] \\ \\ S_\chi = \frac{1}{2}\sum_x \overline{\chi}(x)\sum_{\mu=1}^{4}\eta_{\mu x}(U_{x,\mu}\,\chi_{x+\mu} - U^\dagger_{x-\mu,\mu}\,\chi_{x-\mu}) + am_0\sum_x \overline{\chi}_x\chi_x \\ \\ S_\phi = -\kappa\sum_x\sum_{\mu=1}^{4}[\phi^\dagger_x\,U_{x,\mu}\,\phi_{x+\mu} + \phi^\dagger_{x+\mu}\,U^\dagger_{x,\mu}\,\phi_x] \end{array}} \tag{4.7}$$

4.3.2 Properties of the model

The strongly coupled 4D compact U(1) lattice gauge theory with fermion and scalar fields exhibits some interesting non-perturbative properties[19]. We first point out that the model includes some other known theories. For example at $\beta = 0$ we recover the chiral phase transition seen in the Nambu-Jona-Lasinio model and at $\kappa = 0$ we reach the standard QED theory. Another noticeable fact is that one can construct for the pure gauge theory a non-asymptotic free and non-trivial continuum limit.

However our main interest lies in the more realistic case where both scalar and fermion fields are included. A critical point has been observed at $\beta = 0.64$[14]. When this point is approached from the phase where the chiral symmetry is spontaneously broken the mass am_F of the fermion scales. As expected from the shielded gauge mechanism this fermion, composed of the fundamental fermion and scalar fields is unconfined. The nature of the continuum limit taken at this point is not known yet but it might be possible to obtain a non-perturbatively renormalizable theory. Nonetheless the requirement of renormalizability is very stringent for four dimensional systems. The work presented in this thesis will then consider complementary studies of this model on a three dimensional lattice. The aim is to give further precisions about how the mechanism works.

Part III

Study of the $\chi U \psi$ model in three dimensions

The mechanism of dynamical symmetry breaking which has been introduced relies on four-fermion theories which, at strong coupling, don't depend on the dimensions of the lattice [12]. Four dimensional models have been intensively studied and as mentioned earlier the $\chi U \psi$ model gave promising results with respect to the continuum limit. However the non-perturbative treatment meets some difficulties in 4 dimensions due to ultra-violet divergences. The Nambu Jona-Lasinio model which first introduced dynamical symmetry breaking had already to face the same problem: the cut-off cannot be removed from the scattering amplitudes. However its dependence on them turns out to be only logarithmic and the model could then be employed as a low-energy effective theory for the strong interactions.

The problems caused by ultraviolet divergences leads us to study the model in lower dimensions to test the basic ideas. The studies of 2D models which are exactly solvable gave very useful results. For example the Gross-Neveu model, O(2N) symmetric and with a scalar-scalar 4 fermion interaction, displayed both dynamical mass generation (breaking down a discrete $\psi \rightarrow \gamma_5 \psi$ chiral symmetry) and asymptotic freedom - the two keys for QCD. Nonetheless it is impossible in this framework to break continuous rigid symmetries since the existence of Nambu-Goldstone bosons is precluded by Coleman's theorem (all local operators which are non-singlet under a continuous symmetry group must have a zero expectation value).

3D models are then the natural place to try to build a first complete mechanism whish generate massive fermions in the continuum [15].
We have to assume an infinitely strong coupling ($\beta = 0$) to begin with. In this regime our mechanism remains unchanged but it is interesting to note that it then act on a model which is in the same universality class as the 3D Gross-Neveu model - which is non-perturbatively renormalizable [16][13]. We don't know precisely what happens when the coupling gets finite (but still very large since in addition to the shielded gauge mechanism's requirements the 4-fermion theory is not renormalizable in the weak coupling expansion for 3D models). The critical behaviour of the physical quantities has also to be studied.

The purpose of the following simulations is to establish the phase diagram of the model. This work is based on the analysis of the Lee-Yang zeros of the partition function which is described below.

Chapter 5

Method

The model which has been introduced in the previous chapter is now investigated with tools of statistical physics. Starting from the action defined in section (4.3.1) we define the partition function of the system and can then explore its *thermodynamical* properties. The main objective is to determine the phase diagram of the system at strong and intermediate gauge coupling. This provides the indispensable information on the behaviour of the mass generation mechanism. We find out where the continuum limit is approachable and can also determine various features such as the universality class of the critical line which joins the pure QED theory.

We will explain below the method which has been used and which rests on the Lee-Yang approach. A theorem has been established which shows how the study of the equations of state and phase transitions can be completed just by looking at the distribution of the zeros of the partition function. Although the partition function can be expressed as a polynomial in the fermion mass the determination of these roots is technically non trivial. The numerical procedure which has been designed for this purpose will be described in the second part of this chapter.

5.1 Lee-Yang zeros of the partition function

5.1.1 The Lee-Yang approach

The theorems of Lee and Yang [20] show that phase transitions are manifested in experiment by the occurrence of singularities in thermodynamic functions.

Prior to discuss these two theorems we first have to note that such singularities can only occur because we tend to the idealized thermodynamic limit -

where the volume is expanded to infinity while the number of particles remains the same. Hence as we approach the limit of infinite volume the partition function can develop singularities (due to the fact that the limit function of a sequence of analytic functions is not necessary analytic).

Yang and Lee then stated in the form of two theorems[20] how phase transitions are controlled by the distribution of the zeros of the partition function. They presented their theory in the context of a monoatomic gas. The atoms are assumed to have a finite impenetrable core and their interactions to have a finite range, such that the resulting potential is nowhere minus infinity. Their conclusions can nevertheless be widely generalized to a wide range of systems.

The gas is kept in a finite volume V and thus contains a limited number of atoms M(V). Hence the Grand partition function is a polynomial of finite degree M(V) in the fugacity y.

$$G_V = \sum_{N=0}^{M(V)} \frac{Q_N}{N!} y^N \tag{5.1}$$

From this expression one can obtain the equation of state which can be written in the parametric form:

$$\frac{p}{kT} = \lim_{V\to\infty} \frac{1}{V} \log G_V \tag{5.2}$$

$$\rho = \lim_{V\to\infty} \frac{\partial}{\partial \log y} \frac{1}{V} \log G_V \tag{5.3}$$

Since the coefficients Q_N in eq(5.1) are positive, we note that the polynomial has no real positive roots. If we do not consider the limit of infinite volume then no singularities can occur: p and ρ being analytic functions of y everywhere on the real axis, p would be an analytic function of ρ for all physical values of ρ.

We now expose the two theorems before to discuss how they will lead us to find the phase diagram of the $\chi U \psi_3$ model.

- theorem $\mathcal{I}$: For all positive real values of y, $(\frac{1}{V}) \log G_V$ approaches, as $V \to \infty$, a limit which is independent of the shape of V.
  Furthermore, this limit is a continuous, monotonically increasing function of y. (*it is assumed that the surface area doesn't increase faster than* $V^{\frac{2}{3}}$).

- theorem $\mathcal{II}$: If in the complex y plane a region R containing a segment of the positive real axis is always free of roots, then in this region as $V \to \infty$

all the quantities: $(\frac{\delta}{\delta \log y})^N \frac{1}{V} \log \mathcal{G}_V$ approach limits which are analytic with respect to y. Furthermore the operations $[\frac{\delta}{\delta \log y}]$ and $[\lim_{V\to\infty}]$ commute in R

Hence a thermodynamic phase is defined by any single region R of theorem $\mathcal{II}$. Since in each of these regions the convergence to the limit of infinite volume is uniform we can interchange the order of *lim* and $\frac{\delta}{\delta y}$. This leads in fact to a reformulation of the parametric form of the equations of state. These equations will apply to the whole system provided that the region R includes the entire positive y axis. However if a zero of the grand partition function approaches a point y_0 on the real positive axis, it splits the region R into two regions, R_1 and R_2, in which the theorem $\mathcal{II}$ holds separately.

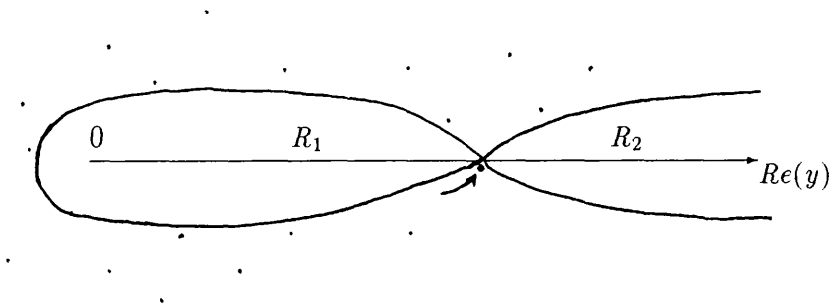

The theorem $\mathcal{I}$ requires $p(y)$ to be continuous - even at $y = y_0$ - but its derivative may be discontinuous. In this last case R_1 and R_2 will correspond to two different phases of the system. Following the discussion of section(1.4) we note that the phase transition will be of first order if a discontinuity is exhibited by the first derivative $(\frac{\partial p}{\partial y})$.

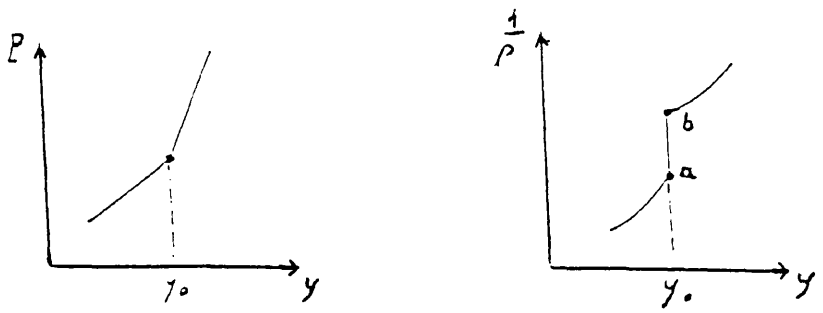

In an other hand, if it is only the second derivative which is discontinuous (or even the third by all means) then one can speak of a continuous phase transition for the observable related to the density $\frac{1}{\rho}$.

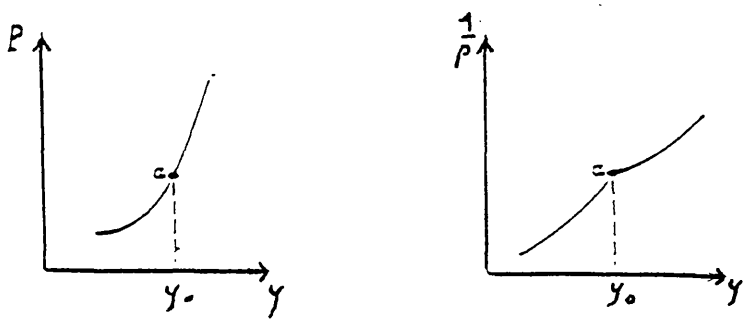

In practice this provides us with a very convenient way to localize phase transitions: At finite volume the partition function exhibits a finite number of complex zeros which lie outside of the real axis - due to the analycity of the function. At increasing volume the sequence of the real parts of the zeros lying nearest to the real axis "pinch" the real axis at a given point where the analytical region is therefore splitted into two parts. Of course this corresponds precisely to the area where the phase transition has to be investigated.

We investigate this region by studying the scaling behavior of the imaginary parts of the critical zeros with increasing volume. For example in a critical region their behavior is given by the scaling law [22]

$$Im(y_i) = A \cdot L^{-\frac{1}{\tilde{\nu}}} \tag{5.4}$$

Where A is a complex number. The critical exponent $\tilde{\nu}$ is directly connected to the order of the phase transition: for a first order transition we would have $\tilde{\nu} = \frac{1}{d}$ where d is the dimension of the lattice. We can also study the universality class to which the region belongs by measuring the quantity: $\delta = \frac{1}{d\tilde{\nu}-1}$. Those tools have been established from experimental observations and the reliability of its results has been confirmed, although no rigorous proof has been given yet.

5.1.2 The partition function as a polynomial in the fermion mass

The partition function which corresponds to our lattice gauge theory is defined by the relation

$$\mathcal{Z}_{\beta,\kappa,m} = \int\int\int [d\chi][d\overline{\chi}][d\phi][d\phi^\dagger][dU]e^{-S} \tag{5.5}$$

The integration over the grassmann variables can be explicitly taken.

$$\int\int [d\phi][d\phi^\dagger][dU]e^{-(S_U+S_\phi)} \int [d\overline{\chi}][d\chi]e^{-S_\chi} = \int\int [d\phi][d\phi^\dagger][dU]e^{-(S_U+S_\phi)} \det M[m, U_\mu(x)] \tag{5.6}$$

where $M[m, U_\mu(x)]$ is the fermionic matrix.

$$M_{x,y}[m, U_\mu(x)] = m\delta_{x,y} + \frac{1}{2} \sum_{\nu=\hat{x}+\hat{y}+\hat{z}+\hat{t}} [U_\nu(x)\eta_\nu(x)\delta_{y,x+\nu} - U_\nu^\dagger(x-\nu)\eta_\nu(x)\delta_{y,x-\nu}] \tag{5.7}$$

This characteristic form of M allows one to write its determinant as a polynomial in the fermion mass for each configuration of the gauge and scalar fields. All our numerical procedure rests on this feature and the starting point is to express this polynomial from which the Lee-Yang zeros can be extracted.

The fermionic matrix of equation(5.7) can be decomposed for a finite lattice as the sum of a diagonal matrix and an anti-hermitian matrix which corresponds to the nearest-neighbour interaction between even and odd sites.

$$M[m, U] = mI_v + \mathcal{H} = \begin{pmatrix} mI_{\frac{v}{2}} & \tilde{M} \\ -\tilde{M}^\dagger & mI_{\frac{v}{2}} \end{pmatrix} \tag{5.8}$$

The subscripts of the square unit matrices denote their size and the $\frac{V}{2} \times \frac{V}{2}$ block matrix $\tilde{M}$ is the even-to-odd site interaction. Hence we can write the fermion determinant as

$$det(M[m]) = det(m^2 + \tilde{M}^\dagger\tilde{M}) = \prod_{i=1}^{\frac{V}{2}} (m^2 + \lambda_i^2). \tag{5.9}$$

where $i\lambda_i$ are the eigenvalues of $i\mathcal{H}$. Since the partition function is the expectation value $< \det(M[m]) >_{U,\phi}$ of this determinant (averaged over configurations which are generated with a probability weight proportional to $\exp -(S_U + S_G)$) we can express equation(5.5) in the form of a polynomial in the fermion mass.

$$\mathcal{Z}_{\beta,\kappa,m} = < \sum_{n=0}^{\frac{V}{2}} a_n m^{2n} > = \sum_{n=0}^{\frac{V}{2}} < a_n > m^{2n} \tag{5.10}$$

The zeros of this polynomial are the Lee-Yang zeros introduced in section (5.1.1).

The corresponding numerical procedure has been designed as follows:

We use an Hybrid Monte Carlo algorithm to obtain an ensemble of thermalised configurations generated with the probability weight $P[U, \phi]$. Then the averaged coefficients $< exp(c_n) >$ of this polynomial are extracted by an iterative method, based on a Lanczos algorithm, which is described in section(5.2.4). We finally obtain the complex zeros by using a standard root-finding routine. As we will see below, during this procedure one must introduce two additional - tuning - parameters in order to neutralise some technical problems which are due to certain features of the distribution of the fermionic determinants in the configuration space as well as the wide range of magnitudes of the coefficients of the resulting polynomial.

The whole process will be repeated at different values of β and κ and by using the Lee-Yang method we will be able to draw the main characteristics of the phase diagram.

5.2 Numerical procedure

5.2.1 Monte Carlo approach

The partition function has been expressed in equation(5.6) as the vacuum expectation values of the fermionic determinant, weighted for each configuration by a probability weight $P[U, \phi]$ proportional to $\exp[-(S_U + S_\phi)]$. All possible configurations being involved, the number of terms in the integrand is quite enormous and the usual methods of calculations cannot handle it.

Monte-Carlo methods solve the problem by selecting only the terms which are not negligible. Clearly a configuration which gives a very high action makes a small contribution to the path integral. In the mean time, configurations for which the action is small are usually so rare that their contribution is not very significant either.

Let $\rho(S)$ be the density of states for a given S. We rewrite

$$\mathcal{Z} = \int \rho(S) e^{-\beta S_{U,\phi}} \det(M[m]) dS \tag{5.11}$$

The configurations which contribute the most to the partition function are those for which $\rho(S)e^{-\beta S_{U,\phi}}$ is maximised [1]. A Monte-Carlo algorithm will find such configurations by the following process: Starting from a given configuration, it will randomly move on to some neighbouring configurations. Then it records which configuration has just been found before to move again. This operation is repeated a numerous number of times until it finds that the probability distribution drawn during the process has become stable. On the ground of this appraisal it can work out a reliable approximation of the integral. This will work if the process is really stochastic ("random walk"). If it was more deterministic then the ergodicity would not be guaranteed and the configurations tested would not be independent from each other. Provided there is enough randomness in the process we can expect that the average obtained will then converge to the correct ensemble average. For a given observable O we write

$$< O >= \frac{1}{N}\sum_{n=1}^{N} O_n + \mathcal{O}(\frac{1}{\sqrt{N}}) \tag{5.12}$$

where $\mathcal{O}(\frac{1}{\sqrt{N}})$ is concerned with the statistical error (which also takes in account the residual correlations between various O_ns).

There are various Monte-Carlo algorithms which all share the same kind of properties. The most important one is the following: If we consider the transition probability $W(\{u\},\{u'\})$ that the algorithm specify from one configuration $\{u\}$ to the next one $\{u'\}$, we must have at the equilibrium

$$e^{-S(\{u\})} = \sum_{\{u'\}} W(\{u\},\{u'\})e^{-S(\{u'\})} \tag{5.13}$$

This is known as the detailed balance condition. It assures that the transition $\{u\} \to \{u'\}$ occurs at the same rate as $\{u'\} \to \{u\}$. This condition fullfiled by all Monte Carlo algorithms can be rewritten as

$$\frac{W(\{u\},\{u'\})}{W(\{u'\},\{u\})} = \frac{e^{-S(\{u\})}}{e^{-S(\{u'\})}} \tag{5.14}$$

5.2.2 Introduction of the updating mass

By 'simulating' the probability distribution of field configurations, Monte-Carlo algorithms allow one to perform numerically enormous path integrations.

[1] $det(M[m])$ doesn't play any role with respect to the discussion above. We will take it in account in the next section.

In the present case however the determinant of the fermionic matrix gives rise to an additional difficulty: The two distributions $P[U,\phi]$ and $\det(M[m])$ don't overlap properly. The region of configuration space where the probability weight peaks is characterised by a negligible contribution of the determinant and vice versa, $P[U,\phi]$ is negligible in the region of large determinant values. Consequently the measurements of m give systematically tiny values due to the vanishing effects of at least one of the two distributions.

The solution to this problem is to introduce a parameter m_0 which shifts the probability weight and makes it to overlap significantly with the distribution of the observable $\det(M[m])$. As we will consider a particular region of the configuration space we will tune m_0 to be as near as possible as the expected value of the lowest zero. We will then perform measurements on the ratios $\frac{\det M(m)}{\det M(m_0)}$ which is then close to the unity.

This parameter is introduced as follow: Since we are looking for the zeros of the partition function, the effects of overall multiplicative factors are not so significant and we can therefore rewrite $\mathcal{Z}$ - for a given β and κ - as

$$\mathcal{Z}_{\beta,\kappa}(m) = \frac{\int [d\phi][dU] \det M(m) e^{-(S_U+S_\phi)}}{\int [d\phi][dU] \det M(m_0) e^{-(S_U+S_\phi)}} \tag{5.15}$$

Hence

$$\mathcal{Z}_{\beta,\kappa}(m) = \frac{\int [d\phi][dU] \frac{\det M(m)}{\det M(m_0)} \det M(m_0) e^{-(S_U+S_\phi)}}{\int [d\phi][dU] \det M(m_0) e^{-(S_U+S_\phi)}} \tag{5.16}$$

$$\mathcal{Z}_{\beta,\kappa}(m) = \int [d\phi][dU] \frac{\det M(m)}{\det M(m_0)} P[U,\phi,m_0] \tag{5.17}$$

Where we set the coefficient $P[U,\phi,m_0]$ to be

$$P[U,\phi,m_0] = \frac{\det M(m_0,U) e^{-(S_U+S_\phi)}}{\int [d\phi][dU'] \det M(m_0,U') e^{-(S_{U'}+S_\phi)}} \tag{5.18}$$

We then designed an Hybrid Monte Carlo algorithm. The partition function is now expressed as the vacuum expectation value of the determinant ratio $\frac{\det M(m)}{\det M(m_0)}$,

averaged over configurations which are generated with the probability weight $P[U, \phi, m_0]$.

$$\mathcal{Z}_{\beta,\kappa}(m) = \langle \frac{\det M(m)}{\det M(m_0)} \rangle_{P[U,\phi,m_0]} \tag{5.19}$$

5.2.3 Shifted expansion of the partition function

From the particular expression of the fermionic determinant in terms of its eigenvalues ($\det(M[m]) = \prod_{i=1}^{\frac{v}{2}}(m^2 + \lambda_i^2)$) we have found an expansion of $\mathcal{Z}$ as a polynomial in the fermion mass (equation 5.10).

There are in fact various forms of expansion of the partition function. For instance it is more suitable in the present case to write a shifted expansion by introducing a mass shift in the determinant:

$$\det(M[m]) = \prod_{i=1}^{\frac{v}{2}}(m^2 - \hat{m}^2 + \hat{\lambda}_i^2) \tag{5.20}$$

where we just substituted $\hat{\lambda}_i^2 = (\lambda_i^2 + \hat{m}^2)$. Hence the partition function's expansion will be written as

$$\det(M[m]) = \sum_{n=0}^{\frac{v}{2}} < b_n > (m^2 - \hat{m}^2) \tag{5.21}$$

It is convenient to write the coefficients in an exponentional form, say $b_n = \exp(x_n)$, since they vary over many orders of magnitude (see figure(5.6)). Moreover the measurements being actually performed on the ratio $\frac{\det(M[m])}{\det(M[m_0])}$ the coefficients x_n will be immediately replaced by $c_n = x_n - \ln\det(M[m_0])$. The polynomial of interest is then given by the expression

$$\mathcal{Z}[m, \beta] = \sum_{n=0}^{\frac{V}{2}} < \exp(c_n) >_{P[m_0,\beta]} (m^2 - \hat{m}^2)^n \tag{5.22}$$

The purpose of this mass shift is twofold. First it is a means to control the reliability of the results by repeating the process above with different choices of $\hat{m}^2$. Clearly the same zeros in m are supposed to appear for adjacent choices of $\hat{m}$ if they are true zeros of the polynomial.

In certain circumstances this technique can also serve to counter the fact that the polynomial coefficients $< \exp(c_n) >_{P[m_0,\beta]} = \exp(\overline{C}_n)$ vary over many orders of magnitude. If $|m^2 - \hat{m}^2|$ is quite small then the last terms of the polynomial will give negligible contributions. This allows the truncation of the polynomial to a

certain order K. The stability of the corresponding zeros can be controlled by then increasing K.

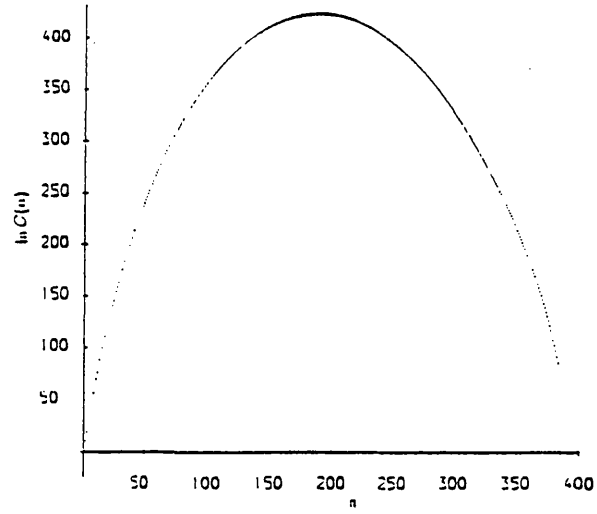

Figure 5.6: The logarithms of the coefficients of the partition function [2]. The C_ns vary in magnitude between e^0 and e^{422} and we therefore express them in exponentional form.

5.2.4 Determination of the coefficients of the polynomial

We now state the iterative method that has been used in order to extract the coefficients of the polynomial.

We see from equation (5.9) - where the determinant has been expressed in terms of the eigenvalues of $\mathcal{H}$ - that for real m^2 the coefficients $\exp(c_n)$ are real positive numbers. We are thus looking for real positive coefficients corresponding to the determinant ratio $\det(M[m])/\det(M[m_0])$ expressed as a polynomial in $(m^2 - \hat{m^2})$. The first step is the Lanczos tridiagonalisation of the hermitian matrix $\tilde{M}^2$ through a similarity transformation

$$X^\dagger \tilde{M}^2 X = T \tag{5.23}$$

[2]These results were obtained for a QCD model (SU(3) gauge group). Nonetheless this wide variation of magnitude is very similar in the U(1) case.

where T is a $\frac{V}{2} \times \frac{V}{2}$ real tridiagonal matrix:

$$T_{\frac{V}{2}} = \begin{pmatrix} \alpha_1 & \beta_1 & & & \\ \beta_1 & \alpha_2 & \beta_2 & & \\ & \beta_2 & \alpha_3 & & \\ & & & \ddots & \beta_{N-1} \\ & & & \beta_{N-1} & \alpha_N \end{pmatrix} \tag{5.24}$$

and X is a series of column vectors $(x_1, x_2, ..., x_N)$. These are the Lanczos vectors which are orthogonal: $x_i^\dagger x_j = \delta_{ij}$. Since the fermionic determinant is invariant under similarity transformations, we can write for example

$$\det(M[m_0]) = \det(\tilde{M}^2 + m_0^2) = \det(T_{\frac{V}{2}} + m_0^2) \tag{5.25}$$

By omitting the last p rows and columns of $T_{\frac{V}{2}}$ we then obtain a new matrix T_p, for which there exists a recursive relation: The Laplace expansion of the determinant gives rise to the equation

$$\det(T_p + m_0^2) = (\alpha_p + m_0^2)\det(T_{p-1} + m_0^2) - \beta_{p-1}^2 \det(T_{p-2} + m_0^2) \tag{5.26}$$

It is convenient to express it in exponential form since we are dealing with variations of several orders: By defining $E_p = \ln\det(T_p + m_0^2)$ we have

$$E_p = E_{p-1} + \ln(\alpha_p + m_0^2) - \beta_{p-1}^2 \exp(E_{p-2} - E_{p-1}) \tag{5.27}$$

with the initial conditions

$$E_0 = 0,\ E_1 = \ln(\alpha_1 + m_0^2) \tag{5.28}$$

Hence we find the value of $\ln\det(M[m_0])$ after $\frac{V}{2}$ iterations of equation (5.24).

The calculation of the characteristic polynomial of $M[m]$ is naturally more complicated. The first steps are identical to those above: writing the determinant in terms of $T_{\frac{V}{2}}$, $[\det(M[m]) = \det(T_{\frac{V}{2}} + m^2 - \hat{m}^2)]$ and using the recursion

$$\det[T_p + (m^2 - \hat{m}^2)] = [\alpha_p + ((m^2 - \hat{m}^2)]\det[T_{p-1} + (m^2 - \hat{m}^2)] - \beta_{p-1}^2 \det[T_{p-2} + (m^2 - \hat{m}^2)] \tag{5.29}$$

Each minor determinant is then expressed as a polynomial in $(m^2 - \hat{m}^2)$:

$$\det[T_p + (m^2 - \hat{m}^2)] = \sum_{n=0}^{p} exp(x_n^{(p)})(m^2 - \hat{m}^2)^n \tag{5.30}$$

This time the recursion (5.27) imposes a recursion on the $x_n^{(p)}$s too. It is written as

$$x_n^{(p)} = x_n^{(p-1)} + \ln[\alpha_p + exp(x_{n-1}^{(p-1)} - x_n^{(p-1)}) - \beta_{p-1}^2 exp(x_n^{(p-2)} - x_n^{(p-1)})] \qquad (5.31)$$

with the initial conditions

$$\begin{array}{ccc} x_0^{(1)} = log(\alpha_1), & & x_1^1 = 0, \\ x_0^{(2)} = log(\alpha_1\alpha_2 - \beta_1^2), & x_1^{(2)} = log(\alpha_1 + \alpha_2), & x_2^{(2)} = 0, \end{array} \qquad (5.32)$$

The coefficients $exp(x_n)$ are obtained after $\frac{V}{2}$ iterations and lead to the c_ns of equation (5.22) which correspond to isolated configurations. We finally average them over our ensemble of thermalised configurations, still using the exponential form, and end up with all the $\overline{C}_n$s after having performed the recursion:

$$\overline{C}^{(k)} = c^{(k)} + \ln(\frac{1 + (k-1)\exp(c^{(k-1)} - c^{(k)})}{k}) \qquad (5.33)$$

where k runs over configurations (we have dropped the subscript n) and the initial condition is simply

$$\overline{C}_1 = c_1 \qquad (5.34)$$

This method is efficient when applied to small lattices (up to 4^3) but it meets additional difficulties from 6^3 lattices. The rounding errors tend to build up exponentially and as a result of this the last vector x_i obtained after each iteration loses the orthogonality with the earliest Lanczos vector of equation(5.22). The usual way to remedy this is to re-orthogonalise: One projects each new Lanczos vector $[x_i \rightarrow x_i - x_j(x_j^\dagger x_i)]$ to make it orthogonal with an earlier vector x_j. However in the present case it would be too costly in storage space and computation time.

Fortunately we can avoid the reorthogonalisation of the Lanczos vectors by using some properties of the Sturm sequences. Our method consists in making the previous algorithm to proceed beyond the $\frac{V}{2}^{th}$ iterations and hence to calculate new Lanczos vectors and α's and β's. After N iterations, we then obtain a tridiagonal matrix $\tilde{T}$ with $\tilde{N}$ eigenvalues $\tilde{\lambda}_i$. Each minor determinant D_n of $\tilde{T} - \mathcal{I}\tilde{\lambda}$ is then extracted through the relations

$$\begin{array}{c} D_n = (\alpha_n - \lambda)D_{n-1} - \beta_{n-1}^2 D_{n-2} \\ D_0 = 1,\ \beta_0 = 0 \\ D_1 = \alpha_1 - \lambda \end{array} \qquad (5.35)$$

Now if we let $\tilde{\lambda}$ be a continuous variable the $D_n(\tilde{\lambda})$'s become analytic functions and their emerging properties can serve to determine accurately the eigenvalues of $\tilde{T}$ matrix.

Loosely, we run the recurrence (5.35) with an arbitrary value of λ. We note that the sign of a given $D_n(\tilde{\lambda})$ might be opposite to the one of the previous $D_{n+1}(\tilde{\lambda})$. As we perform the recursion again for neighbouring values of $\tilde{\lambda}$ the total number of sign changes from D_1 to D_N might be different. It means that at least one of the D_ns changed sign between the two $\tilde{\lambda}$s. Since they are analytic functions their graphs necessarily crossed the absisse axis. This is how one can track the precise value of $\tilde{\lambda}$ at which D_N vanished: Simply by running the D_n sequence for closer and closer values of $\tilde{\lambda}$ until the total number of sign changes increases. We can then identify each $\tilde{\lambda}_i$ thanks to a theorem which shows that if we obtained i sign changes then we are between the i^{th} and the $(i+1)^{th}$ eigenvalue of $\tilde{T}$. These is how the $\tilde{\lambda}_i$'s are found.

Having found the eigenvalues of $\tilde{T}$ we can deduce from them the eigenvalues of M^2: It has been found empirically that if N is sufficiently large the λ's will all converge toward some of the $\tilde{\lambda}$'s. The task now is to identify the spurious eigenvalues $\tilde{\lambda}_s$ which are not eigenvalue of M^2. One way to do so is to look at the eigenvalues of the matrix $\hat{T}$ formed from the $N-1$ first iterations. Like $\tilde{T}$, $\hat{T}$ will contain the eigenvalues of M^2. However the spurious eigenvalues will have changed: indeed the last component of their eigenvectors are large and they are therefore greatly affected by removing the last α and β. Hence the true eigenvalues are those that M^2 shares with both $\tilde{T}$ and $\hat{T}$.

Once we have found the eigenvalues of the fermion matrix, we define coefficients $r_k^{(n)}$ through the expansion.

$$\det(M[m]) = \prod_{i=1}^{n}(m^2+\lambda_i^2) = \sum_{k=0}^{n} r_k^{(n)} m^{2k} \tag{5.36}$$

It gives rises to the iteration

$$r_k^{(n+1)} = r_k^{(n)}\lambda_{n+1}^2 + r_{k-1}^n \tag{5.37}$$

with $r_0^{(1)} = \lambda_1^2$ and $r_1^{(1)}$. After $\frac{V}{2}$ of these iterations one finally obtains the coefficients $\exp(c_n) = r_n^{(\frac{V}{2})}$.

Chapter 6

Results

6.1 Introduction

The procedure defined in chapter 5 has been applied to the U(1)gauge-fermion-scalar model on a three dimensional lattice. We present the results of our numerical simulations which has led, in collaboration with a group in Aachen [1], to the determination of the phase diagram for the system.

Measurements of the expectation value of the fermionic determinant were performed at various values of β (on a three dimensional lattice β is now related to the gauge coupling constant through the relation $\beta = \frac{1}{ag^2}$) and κ. We then obtained the distribution of the zeros of the partition function in the complex mass plane for various regions of the $\beta - \kappa$ plane.

The graphs displayed in the following sections show the zeros in the upper-right quarter of the complex mass plane ($Im(\mathcal{Z})$ and $Re(\mathcal{Z})$ positive). Nonetheless the complete distribution covers the whole complex plane: the complex conjugates of these zeros and their negative are also zeros of the polynomial.

The zeros of the partition function were first determined on a 4^3 lattice. The update mass in the Hybrid Monte Carlo generation of the ensemble was chosen to be in the vicinity of the expected real part of the lowest zero. We used $am_0 =$ 0.005, 0.02 or 0.05. This preliminary investigation revealed the main properties of the phase diagram. We could identify three main regions as discussed below.

We then generated new ensembles on 6^3, 8^3 and 10^3 lattices in order to perform a finite size scaling analysis on the zeros closest to the real axis [2]. This analysis of

[1] In particular the work of W.Franzki from the *Institut für Theoretische Physik*[21]

[2] We used also 12^3 lattices in regions where the gauge coupling was weak

the scaling behavior of these zeros determines the order of the phase transitions and allows us to obtain a precise localisation of the critical points.

This work will be presented in the following order: We first discuss measurements obtained from simulations on the 4^3 lattice at strong and intermediate couplings. This provides an introduction to the way that one can extract qualitative information on the thermodynamic properties of the system by looking at the distribution of the zeros and their response to a change in the physical parameters β and κ.

We then summarize our results on larger lattices and present the finite size scaling analysis and the critical exponents found. Finally we describe our interpretation of these measurements via the phase diagram and discuss its main characteristics as well as their physical implications.

6.2 Strong coupling on a 4^3 lattice.

The line along the κ axis at $\beta = 0$ is useful in checking the validity of our method since the model can then be rewritten exactly as a four fermion theory [19] and we recover the $(2+1)$ Gross Neveu model [3].

Since the zeros are imaginary in this region we took a low updating mass, $m_0 = 0.005$. The distribution of the zeros was first determined at $\kappa = 0.33$ and is shown in Fig. 6.1.

The zeros are observed to be purely imaginary and evenly spaced along the imaginary axis. The lost of linearity observed above the 28^{th} zero is due to the fact that the coefficients controlling these zeros are not well determined. These zeros would be better determined if more measurements were averaged over. This feature has no major consequences since we base our finite size scaling analysis only on the zeros which lie near to the real axis.

The equal spacing of the zeros does allow a simple method for the determination of the fermion condensate $< \overline{\chi}\chi >$. We can parameterize the zeros as

$$y_n = \pm\imath(a + nb) \tag{6.1}$$

[3]This model is the first to disclose that 4-fermion theories are in fact renormalizable in the $\frac{1}{N}$ expansion in $d = 1 + 2$. It then revealed information on non-pertubative possibilities [16].

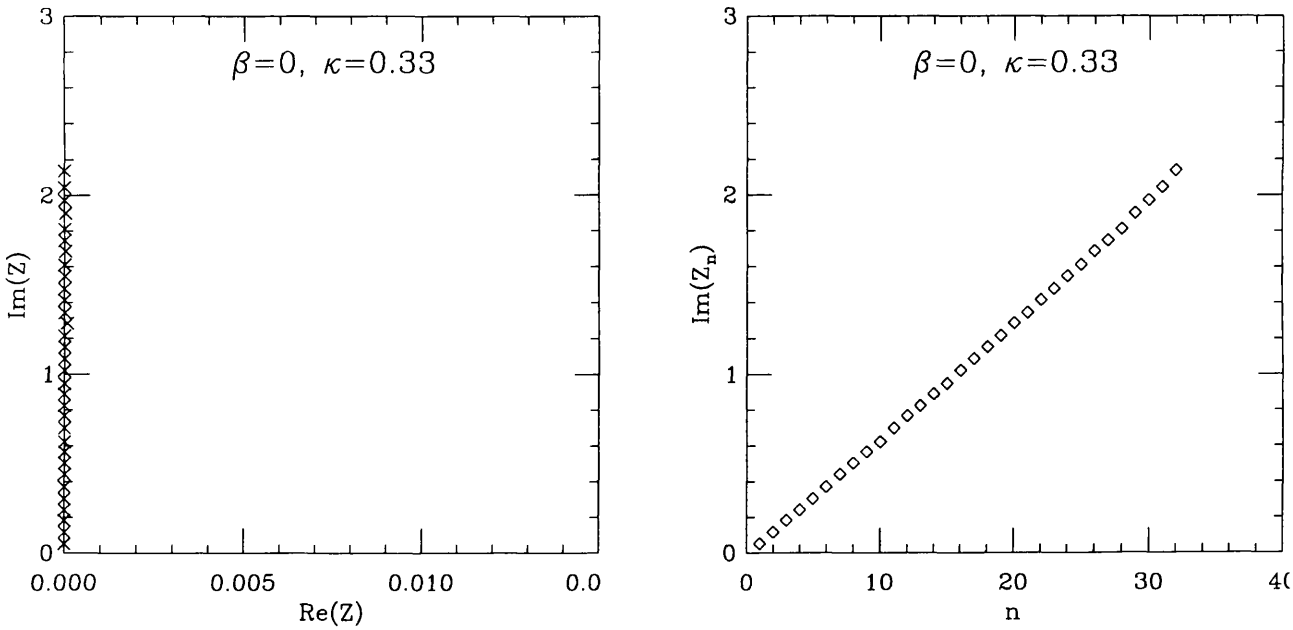

Figure 6.1: The zeros of the partition function in the complex mass plane for a 4^3 lattice at strong coupling and $\kappa = 0.33$. 2500 measurements were made to determine the averaged characteristic polynomial. On the right hand side the imaginary part of the n^{th} zero is plotted against n.

Then the relation (5.22) leads us to

$$\ln \mathcal{Z} = \sum_{n=0}^{\frac{V}{2}} \ln(m^2 + (a+nb)^2) \tag{6.2}$$

$$= V \int_0^{\frac{1}{2}} \ln(m^2 + (a+Vbx)^2) dx \tag{6.3}$$

for the grand canonical partition function and for the fermion condensate:

$$< \overline{\chi}\chi > = \frac{1}{V}\frac{\partial}{\partial m} \ln \mathcal{Z} \tag{6.4}$$

$$= \frac{2}{Vb}(\arctan(\frac{Vb/2+a}{m}) - \arctan(\frac{a}{m})) \tag{6.5}$$

In order that we have a first order phase transition in the infinite volume limit at $m = 0$ the edge a must scale with some positive power of the inverse of V and b must scale inversely with V. As we show below, simulations on larger lattices show that in this region of κ they both scale as $1/V$. Therefore if we introduce in eq(6.5) the following expressions: $a = \frac{a'}{V}$, $b = \frac{b'}{V}$ and go to the limit $V \to \infty$ (

a'/V becomes negligible), we obtain

$$< \overline{\chi}\chi >= \frac{2}{b'} \arctan(\frac{b'}{2m}) \tag{6.6}$$

Finally by taking the limit $m \rightarrow 0$ we have the simple relation:

$$< \overline{\chi}\chi > \rightarrow \frac{\pi}{b'} \tag{6.7}$$

Figure 6.1 corresponds to a spacing $b = 0.058 \pm 0.003$ between each zeros. Hence, assuming that a and b scale with the volume, the fermion condensate at the point $\beta = 0$ and $\kappa = 0.33$ is equal in lattice units to $< \overline{\chi}\chi >= 0.841$. These results are consistent with the prediction given by the strong coupling expansion [23].

Further simulations at $\beta = 0$ have been performed by the Aachen group. They confirm this first order behaviour at $\kappa = 0.33$. At larger κ (around $\kappa = 1$) they find a transition to second order critical behaviour as expected for the Gross-Neveu model. Their results in this region are discussed below.

6.3 Intermediate couplings on a 4^3 lattice.

Fig 6.2 shows the distribution of the zeros on a 4^3 lattice at various values of β and κ.

Consider the behaviour of the zeros along the line $\kappa = 0.33$ in the $\beta - \kappa$ plane. At $\beta = 0$, as discussed above, the zeros are imaginary and equally spaced. As β increases to 1.0 we see the same behaviour in the zeros closest to the origin but at $\beta = 1.0$ we have a signal that some of the zeros are developing a non-zero real part. At $\beta = 1.25$ the lowest zero, the edge singularity, has a non-zero real part. We have checked this result by measuring the zeros on two different ensembles: one developed at update mass 0.05 and the other at update mass 0.005. The edge singularity is the same in both.

We also note that along this line, the imaginary part of the edge singularity increases with β. In addition, for $\beta < 1.25$ the lowest zeros of the partition function are, to a good approximation, still evenly spaced along the imaginary axis. However the spacing b between each zero has however increased and therefore the fermion condensate is decreasing.

At $\beta = 1$ for $\kappa = 0.15, 0.33$ and 0.45 we also find the edge singularity to be imaginary and increasing with κ. Again there is a signal that the zeros are developing a real part at larger κ

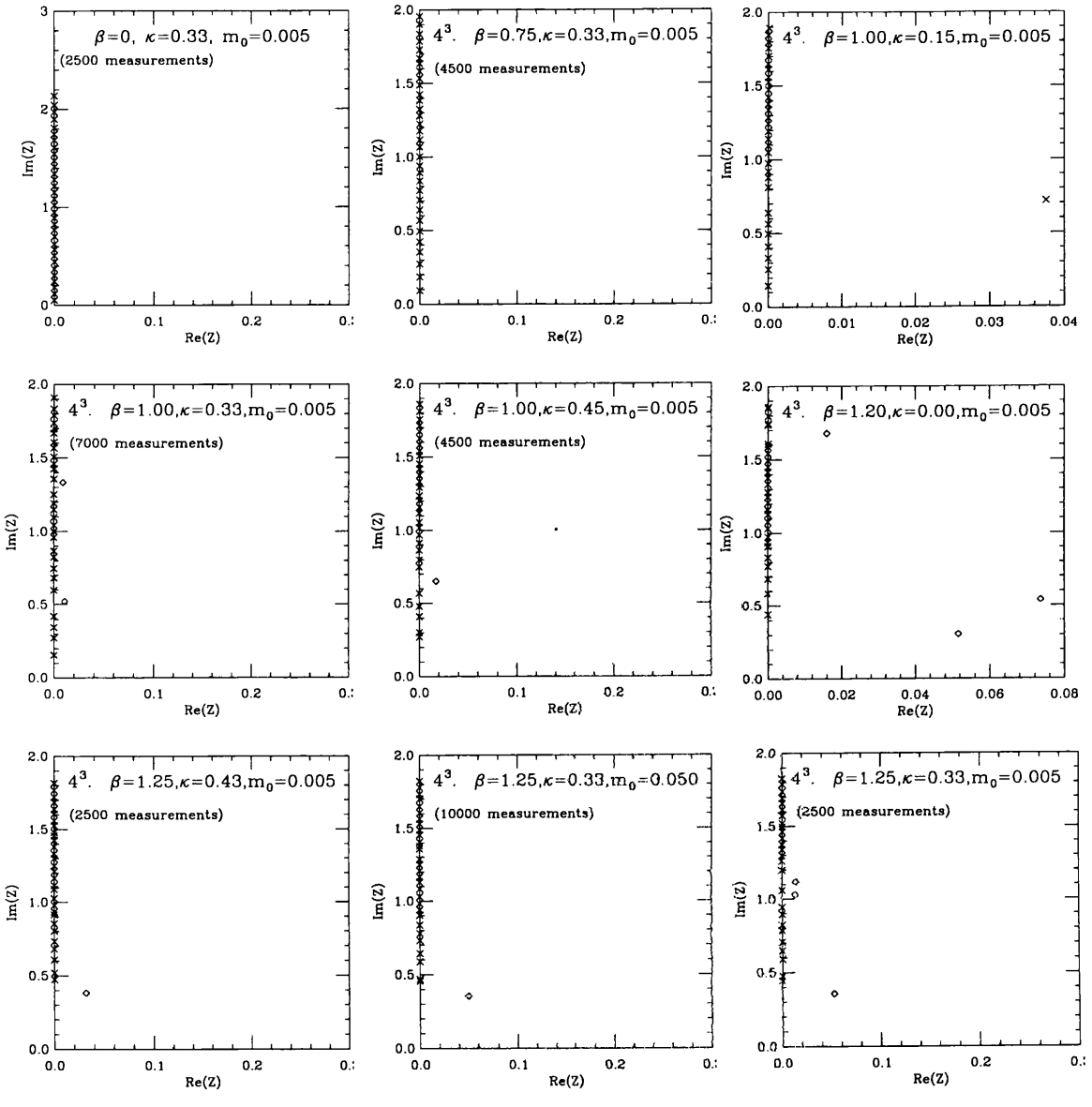

Figure 6.2: The distribution of the Lee-Yang zeros on a 4^4 lattice at various values of β and κ

The above results indicate the possibility of a transition around β of 1.25 (at $\kappa = 0.33$) from a region with a first order chiral transition at $m = 0$ to a region with different critical behaviour. Thus for $\beta < 1.25$ we have two regions with different chiral critical behaviour separated by a line or curve starting at $\kappa = 1$ for $\beta = 0$ and terminating at $\kappa = 0$ for $\beta \approx 1.25$. In one region, the Nambu phase, the chiral symmetry appears to be strongly broken. In the other, the Higgs phase, it is either zero or very small[4].

The measurements on the 4^4 lattice have signalled the dominant critical features of the model in its chiral limit. More detailed analysis must depend on simulations on larger lattices and on finite size scaling.

6.4 Finite size scaling of the zeros at strong coupling.

Fig. 6.3 shows the finite size scaling of the edge singularity for different values of κ.

The lowest zeros $Z_c(L)$ should scale with the lattice size L (on an L^3 lattice) as

$$Z_c(L) - Z_c(\infty) = AL^{-\frac{1}{\tilde{\nu}}} \tag{6.8}$$

where A is a complex number. [22] This was originally established for the case of a continuous phase transition and can also be extended to a first order transition. It requires that the real and imaginary part of the zeros should scale independently with the same exponent. In particular

$$ImZ_c \sim AL^{-\frac{1}{\tilde{\nu}}} \tag{6.9}$$

Since there is no divergent correlation length the exponent (namely $\tilde{\nu}$) is determined only by the actual size of the system. A first order phase transition corresponds to $\tilde{\nu} = \frac{1}{3}$.

We took the lowest zero in the distribution at each volume and plotted the the logarithm of imaginary part and their real part against the logarithm of the lattice size L (see Figure 6.5).

[4]More detailed analysis by the Aachen group on large lattices with high statistics now shows that, in the chiral limit, the condensate is zero in the Higgs phase.

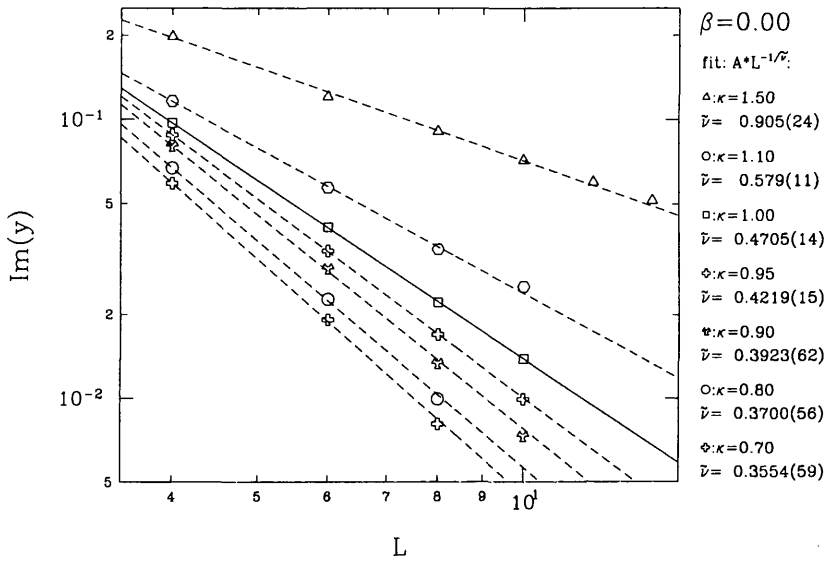

Figure 6.3: Finite size scaling behavior of the lowest zeros of the partition function for various values of κ at strong coupling.(From simulations performed in Aachen))

At strong coupling the edge singularity signals a first order phase transition for $\kappa < 1.0$. This is particularly clear at $\kappa = 0.70$ where the critical exponent is equal to $0.36 \simeq \frac{1}{d}$ (d is the dimension of the lattice).

At $\kappa = 1.00$, $\tilde{\nu} = 0.47(5)$ which is consistent with a continuous phase transition. For $\kappa > 1.0$ the chiral condensate is small and consistent with zero whereas for $\kappa < 1$ it is clearly non-zero.

Moreover the exponent $\delta = \frac{1}{d\tilde{\nu}-1} = 2.4(10)$ and therefore indicates [21] that this point belongs to the same universality class as the chiral phase transition observed in the (2+1) Gross-Neveu model[14].

6.5 Finite size scaling of the zeros at intermediate couplings.

At fixed β and κ we generated ensembles on lattices of increasing volume. As stated above, the critical zeros in the complex plane should obey the scaling law:

$$Z_c(L) - Z_c(\infty) = AL^{-\frac{1}{\tilde{\nu}}} \tag{6.10}$$

where A is a complex number. We took the lowest zero of the distribution for each volume, V, and plotted its imaginary part and real part against the lattice length ($L = \sqrt[3]{V}$) on a log-log plot.

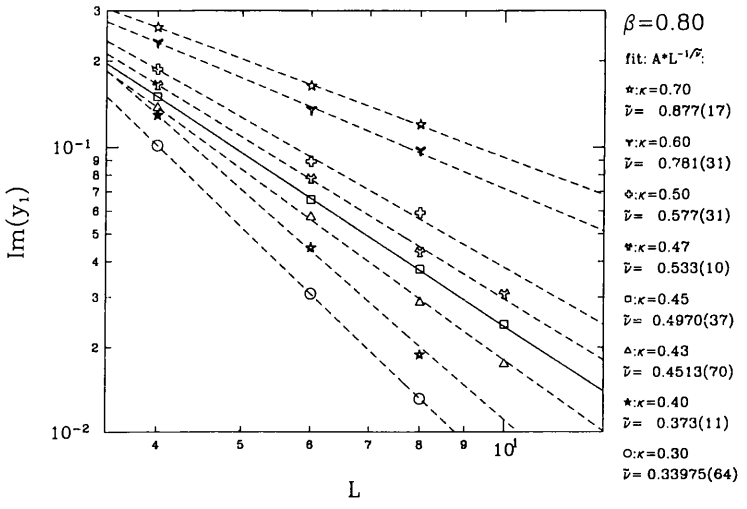

Figure 6.4: Fitting of the imaginary and real part of the edge singularity for increasing lattice volumes. On a logarithmic scale the curve appears to be a straight line.

Fig. 6.4 shows the scaling behaviour of the edge singularity at $\beta = 0.8$ for various values of κ. This set of results should be compared with the equivalent set at strong coupling, Fig 6.3.

Whereas at strong coupling we found the critical $\kappa_c = 1.00(05)$, at $\beta = 0.8$ we find the same qualitative features but with $\kappa_c = 0.45(2)$ We therefore have a critical line extending into the $\beta - \kappa$ plane separating the Higgs phase (large κ) from the Nambu phase.

However our simulations on the 4^3 lattice did indicate the possibility of a further transition at $\beta \approx 1.25$ and $\kappa \approx 0.33$ to a region with different critical behaviour (i.e, the region $\beta > 1.25$ and $\kappa < 0.3$).

In that region the edge singularity develops a non-zero real part. Fig.6.9 shows the distribution of the zeros on $6^3, 8^3$, and 10^3 lattices. We found the real part of the edge singularity to be zero on the 10^3 lattice but, within our statistical errors, it equally well could be non-zero but very small.

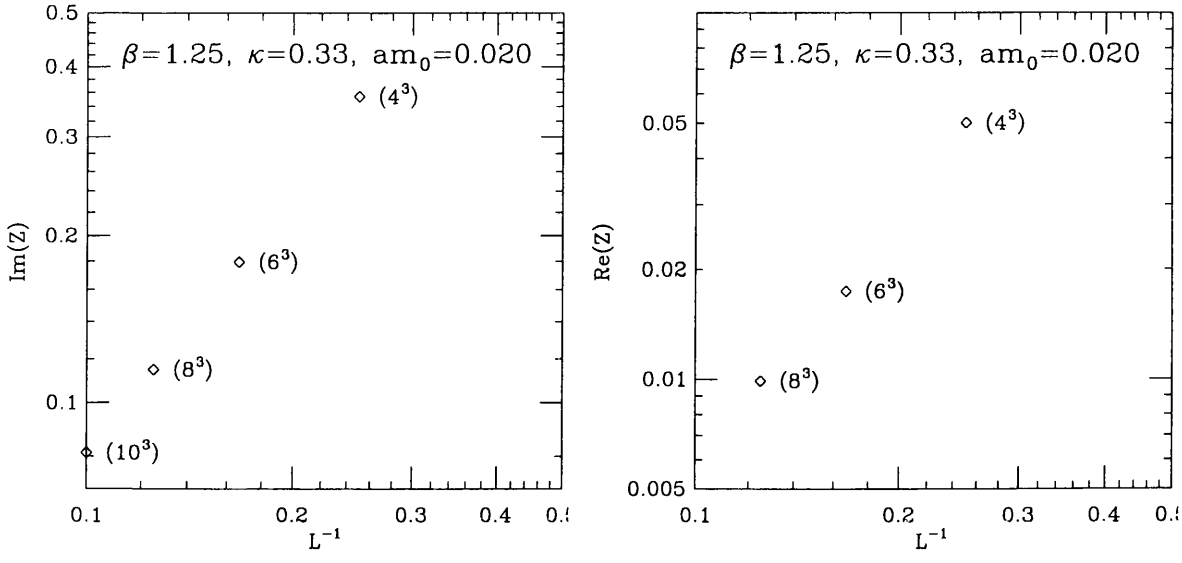

Figure 6.5: Fitting of the imaginary and real part of the edge singularity for increasing lattice volumes on a log-log plot at $\beta = 1.25$ and $\kappa = 0.33$.

Fig. 6.5 shows the scaling behaviour of the real and imaginary parts of the edge singularity. We have also included our data on the 4^3 lattice.

The real part of the edge singularity on the 10^3 lattice is predicted to be ≈ 0.005 which we believe would be consistent, within our errors, with that of Fig.6.9.

The critical exponents were found to be $\tilde{\nu}_{Re} = 0.4276$ and $\tilde{\nu}_{Im} = 0.4707$. This is consistent with a second order phase transition. Simulations at larger values of β show that finite size effects are large at weak coupling. We find the critical exponents at weak coupling to be second order. Fig.6.6 shows the scaling behaviour of the zeros at $\beta = 2.0$ and $\kappa = 0.15$. There the critical exponent $\tilde{\nu} = 0.71$. The phase diagram at weak coupling is discussed in more detail below.

6.6 Fine tuning of κ critical

We discuss here a technique which leads to the fine tuning of the κ_c at which, for fixed β, we move from the Nambu phase to a region with second order critical behaviour. The technique again depends on the scaling behaviour of the zeros of the partition function.

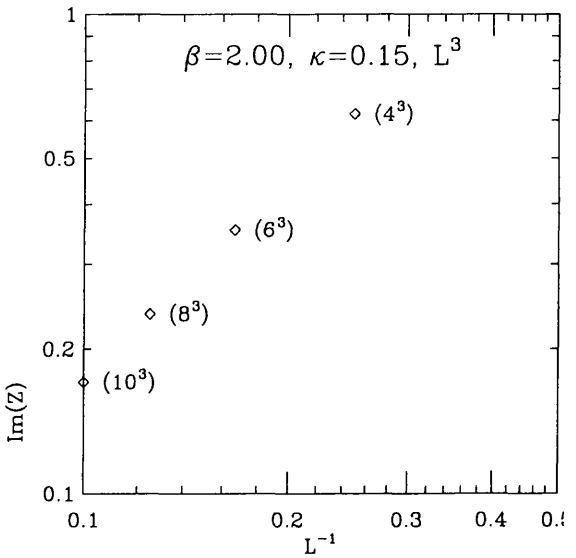

Figure 6.6: The finite size scaling of the imaginary part of the critical zeros at weak coupling. The critical exponent $\tilde{\nu}$ at $\beta = 2.0$ and $\kappa = 0.15$ is 0.71

However we now consider a lattice of constant volume: it is the value of the hopping parameter κ which will be the variable.

We determined the distributions of the zeros on an 8^3 lattice with β fixed at 1.25 at various values of κ; from $\kappa = 0.75$ to $\kappa = 0.33$ where the critical point is expected.

The distributions of the zeros for $\kappa = 0.75$, 0.43, 0.40 and 0.35 are shown in Figs.6.10 and 6.11.

We are "tracking" a critical line which separates the Nambu phase where the chiral symmetry is broken via a first order transition and a phase where the transition is second order and the chiral condensate is small (zero). In the latter phase we assume that the imaginary part of the edge singularity has a κ dependence

$$Im(Z) = A + B(\kappa - \kappa_c)^{\nu}. \tag{6.11}$$

We found a best fit to the κ dependence by considering A, B, κ_c and ν as free parameters. The best fit is shown in Fig.6.7. It gave $\kappa_c = 0.348$ and $\nu = 0.488(6)$

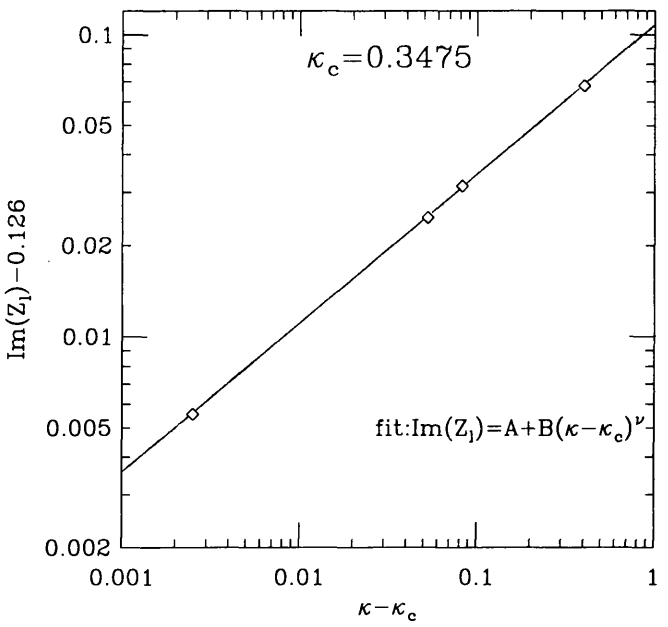

Figure 6.7: final fitting after having determinated κ_c numerically.

6.7 Phase diagram

Having reviewed the main techniques that have been employed in this investigation we now describe the phase diagram of the $\chi U \psi_3$ model. In this section we make use of the more detailed results regarding the mass am_F of the fermion state $F = \psi^\dagger \chi$ and the fermion condensate obtained in the Aachen simulations [21].

The edge singularity, at $\beta = 0$, displays a first order phase transition: We have for example at $\kappa = 0.7$, $\tilde{\nu} = 0.356$ ($\rightarrow 1/3$).

Below this point the chiral symmetry is broken and measurements of the fermion condensate $< \overline{\chi}\chi >$ give non-zero values. However at $\kappa = 1.1$ $< \overline{\chi}\chi >$ vanishes and the scaling behaviour of the zeros indicates a second order phase transition. This critical point corresponds to the chiral phase transition observed in the Gross Neveu model and it would be interesting to pursue further studies of the scaling of zeros at this point. From the critical exponent $\delta = \frac{1}{d\tilde{\nu}-1}$ we might find that this point is universal.

A critical line extends into the β, κ plane separating the regions with first and second order chiral transitions. This critical line starts from the point $(\beta, \kappa) =$

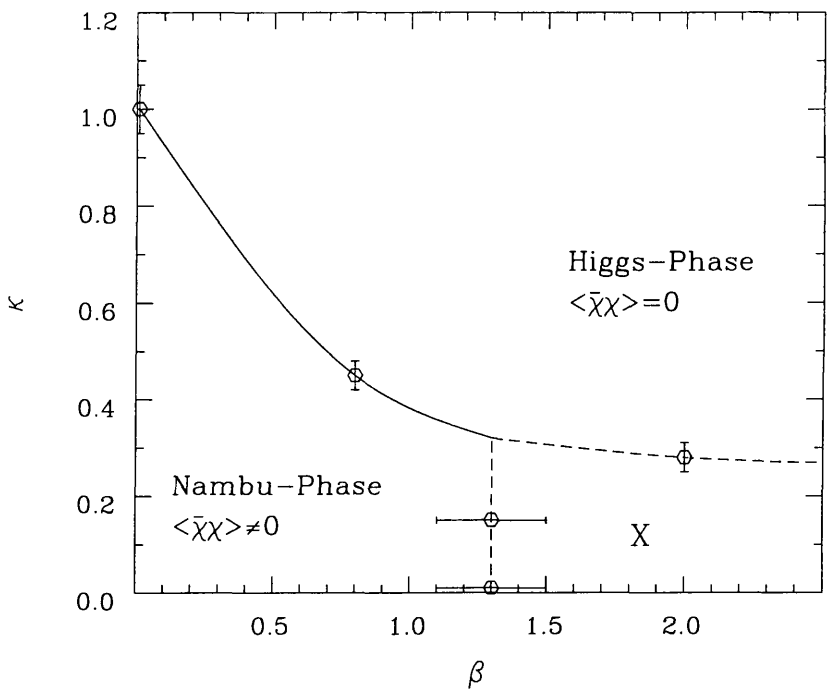

Figure 6.8: Phase diagram of the 3 dimensional $\chi U \psi$ model

$(0, 1.1)$ and passes through the points $(0.8, 0.45)$, $(1.25, 0.35)$ and may extend to $\beta = \infty$ for small values of κ.

Below this critical line, the zeros of the partition function are imaginary and the scaling of their linear density indicates a first order transition similar to the scaling of the edge singularity as discussed above. The fermion condensate as well as the mass am_F of the fermion state $F = \psi^\dagger \chi$ are non-zero: This is the phase where the dynamical symmetry breaking operates. Both χ and ψ fields are confined and in the limiting case $\beta = 0$ the χ and F states become identical. For this reason, this phase is referred to as the Nambu phase.

Above the critical line, the Higgs mechanism operates. The zeros of the partition function are still imaginary but the behavior of the physical observables is quite different from that of the previous case. Both the fermion mass and the fermion condensate vanish. All physical states are gauge invariant and the U(1) charge is screened by the scalar condensate. Provided we choose the gauge charge

to be equal to one, we also recover, for weak coupling, the U(1) vector boson and the Higgs boson. We call this phase the Higgs phase.

There is a third phase "X" whose nature has not been understood thoroughly yet. It lies below the critical line at weak coupling. Here the zeros are complex (i.e. have a nonzero real part), and, as shown in Fig.6.6 the edge singularity has a scaling behaviour corresponding to a second order transition. We believe that it is the nonzero real part of the zeros which distinguishes this phase from the Higgs phase.

In addition the fermion condensate $\overline{\chi}\chi$ is small or zero but the fermion mass am_F is quite big (in the Higgs phase am_F is zero).

The transition to the Higgs phase is therefore difficult to investigate. Further investigations have to be performed. Indeed it is not clear from the finite size scaling of the zeros that there is a change in critical behaviour for $\beta \geq 1.3$.

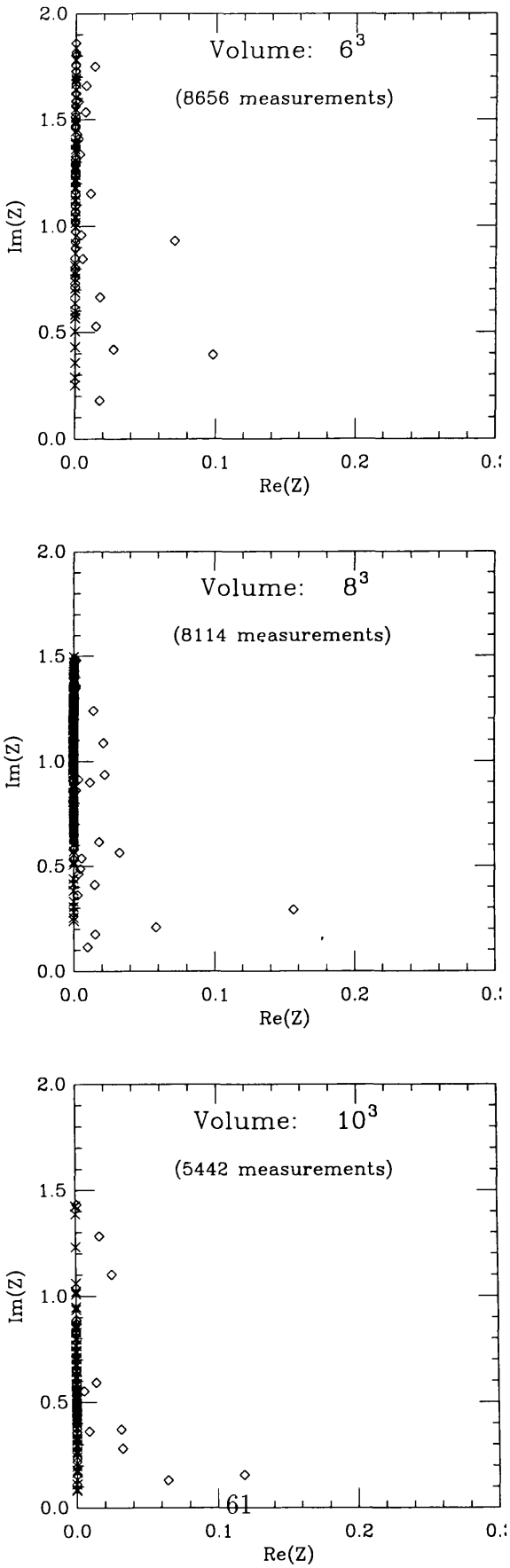

Figure 6.9: Distribution of the zeros at $\beta = 1.25$ and $\kappa = 0.33$ for different lattice volumes

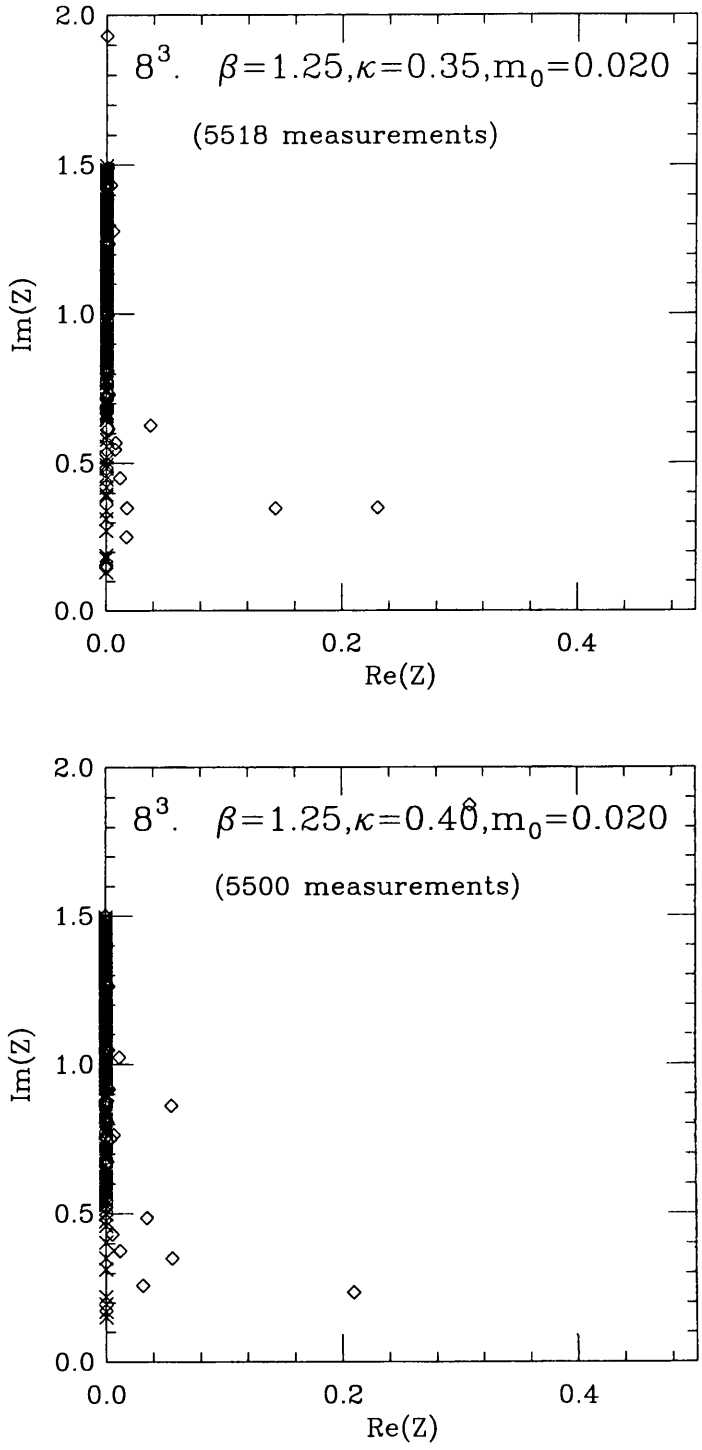

Figure 6.10: distribution of the complex zeros on an 8^3 lattice at $\beta = 1.25$ for $\kappa = 0.35$ and 0.40.

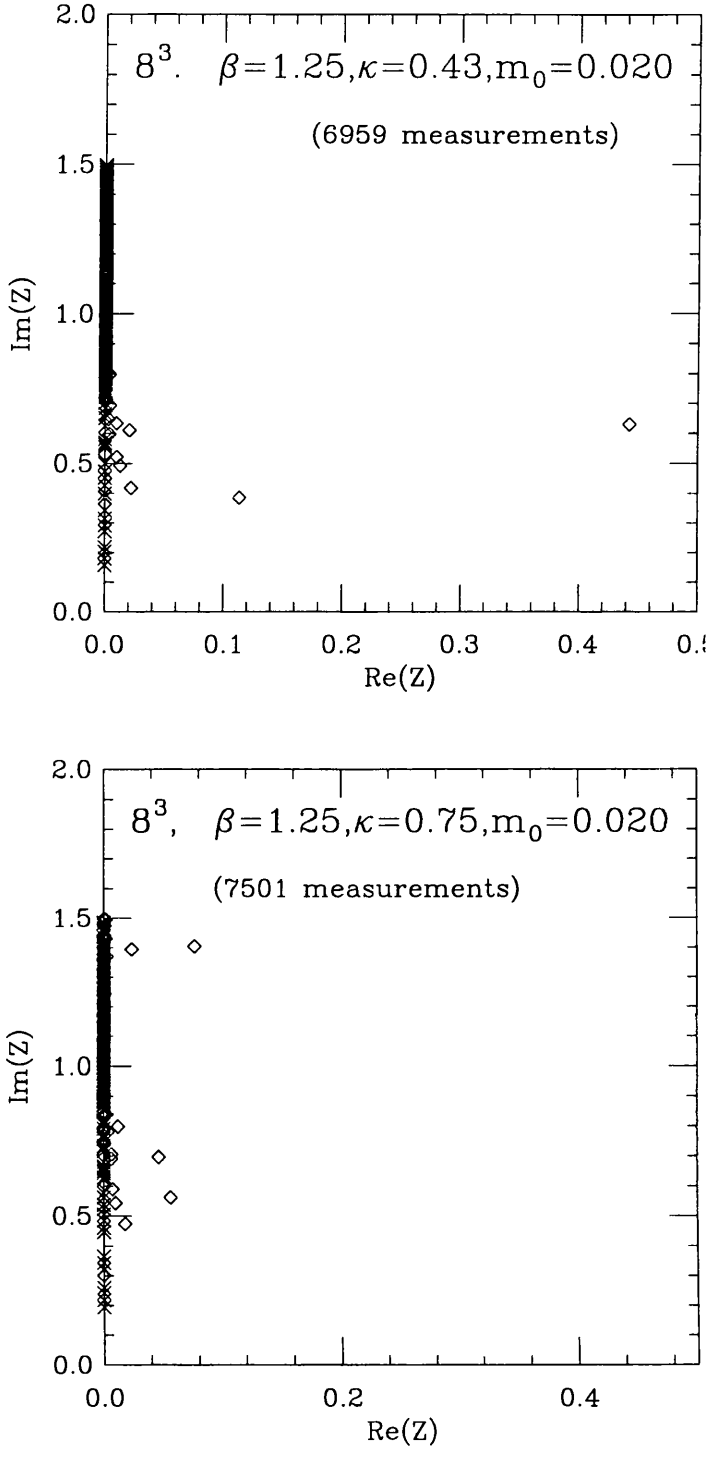

Figure 6.11: distribution of the complex zeros on an 8^3 lattice at $\beta = 1.25$ for $\kappa = 0.43$ and 0.75.

Chapter 7

Conclusion

The study of the zeros of the partition functions proved once again to be a powerful tool in the investigation of the phase structure of a lattice field theory. Although the computing power available is often a major limitation for this kind of study, the Hybrid Monte Carlo scheme which has been introduced here enabled us to extract the most valuable data on the $\chi U \psi_3$ model , at strong and intermediate coupling, and revealed crucial properties of the system with respect to the generation of the fermion mass.

The model displays a mechanism of dynamical fermion mass generation which is analogous to those of the Gross-Neveu model at strong coupling and persists at finite values of β. As κ increases, the order parameter vanishes and the chiral symmetry is then restored. The scaling behavior of the corresponding critical line gives evidence of a second order phase transition where the fermion mass is observed to tend continuously to zero. Furthermore the points along this chiral transition line which correspond to $\beta = 0$ and $\beta = 0.8$ both belong to the same universality class as the (2+1) Gross-Neveu model and we can expect that it would be true for the whole transition line - in which case the model would be non-pertubatively renormalizable in the continuum limit. However some deviation, along the transition line, have been observed and further measurements have to be performed. Clearly the non-perturbative renormalizability of the model is a matter which will require a rigorous verification.

Further investigations have also to be carried out on the region of weak gauge coupling and small κ. In particular the transition within the Nambu phase at which the fermion mass vanishes is not well explained. This transition line - which joins at $\kappa = 0$ the pure QED theory - requires to be understood a wider scale

analysis of the physical observables by means of larger lattices. This is currently being studied within another project.

Bibliography

[1] R.E.Marshak, *Conceptual Foundations of Modern Particle Physics*, World Scientific (1993).

[2] S.Weinberg, *The Quantum Theory of Fields, Foundations*, Cambridge university press (1993) p.499.

[3] C.Cohen-Tanoudji, B.Diu, Mecanique Quantique, edit. Hermann.

[4] F.J.Dyson, Phys.Rev. 75 (1949) 1736.

[5] C.N.Yang, Selected papers 1945-1980 with commentary, W.H.Freeman, San Francisco (1983) p.563.

[6] K.Wilson, Phys. Rev. D10 (1974) 2445.

[7] F. Wilczek, Remarks on the phase transition in QCD (1992) Proc. IFT Conference on dark matter (1992) Princeton.

[8] M.Le Bellac, *Des phenomenes critiques aux champs de jauge* InterEditions / Editions du CNRS (1988).

[9] R.Shrock, Nuch. Phys. B (Proc. Suppl.) 29B (1992) 124.

[10] K.Cahill, l Phys. Lett. B269 (1991) 129.

[11] Y.Nambu and G.Jona-Lasinio, Phys. Rev. 122 (1961) 345; 124 (1961) 246. Y.Nambu Quasi-supersymmetry, bootstrap symmetry breaking and fermion masses, *in* Proc.Int. Workshop on new trends in strong coupling gauge theories, Nagoya, Japan 1988, ed M.Mando, T.Muta and K.Yamawaki (World Scientific, Singapore, 1989).

[12] I.Lee, R.Shrock, Phys. Rev. Lett. 59 (1987) 14.

[13] B. Rosenstein, B. Warr and S. Park Phys. Rev. Lett. 62 (1989) 143.

[14] E. Focht. J. Jersak. J. Paul, Nucl. Phys. B47 (1996) 709.

[15] B. Rosenstein, B. Warr and S. Park Phys. Rep. 205 (1991) 59.

[16] D. Gross, A. Neveu, Phys. Rev. D10 (1974) 3235.

[17] C.Frick and Jiri Jersak, Phys. Rev. D52 (1995) 340.

[18] I.M.Barbour, G.Salina, *The finite size scaling behaviour of the Lee-Yang zeros in compact lattice QED at non-zero temperature.* - unpublished.

[19] W. Franzki *et al*, Nucl. Phys. B453 (1995) 355.
W.Franzki and J.Jersak, Nucl. Phys. B(Proc. Suppl.) 47 (1996) 663.

[20] C.N.Yang and T.D.Lee, Phys.Rev. 87 (1952) 404.
C.N.Yang and T.D.Lee, Phys.Rev. 87 (1952) 410.

[21] W.Franzki, *Dynamische Erzeugung von Fermionmassen in stark gekoppelten Eichtheorien auf dem Gitter*, Dissertation RWTH Aachen, 1997.

[22] V. Azcoiti *et al.*, Phys. Rev. D51 (1995) 5199.

[23] Jolicoeur, Nucl. Phys. B235 (1984) 455.

[24] I.M.Barbour *et al.*, Phys. Lett. B341 (1995) 355-360.